"Page missing from available version"

I, II,

TABLE OF CONTENTS

LIST OF FIGURES

LIST OF FIGURES
(Continued)

SUMMARY

Methods for introducing optical information directly, without intervening recording and storage steps, into integrated optical data-processing devices are surveyed. The information is taken to be in the form of a one-dimensional variation of intensity across the beam. Physical phenomena that may be utilized, including photorefractive, photochromic, thermooptic, photoconductive, and photovoltaic effects, are evaluated, and the most suitable presently known classes of materials for exploitation of each type of interaction are discussed. A variety of possible device configurations utilizing various interaction phenomena are suggested and general principles are outlined whereby many more device types can be generated. While many plausible methods for direct optical input can be outlined, none can be said to be generally superior, in part because the most feasible scheme for a given application will be strongly dependent on the nature of the input signal and the data-processing operations to be carried out, and in part because of uncertainties concerning the ultimate capabilities of the various classes of photosensitive materials and concerning the compatibility of different optical waveguide materials. A simple experimental device was demonstrated and its operation was analyzed. It involves differential electro-optic phase modulation in pairs of parallel waveguide channels through absorption of signal beam light in a photoconductive surface layer. The phase modulation was converted to an intensity modulation by using an external lens.

INTRODUCTION

Recent years have seen great interest, activity, and progress in the development of optical data-processing devices based on integrated-optics technology. Such devices offer potential advantages in terms of combination of light weight, mechanical rigidity, low operating power, freedom from electromagnetic interference, and high data rates that are hard to achieve in any other way. Since the input data to be processed will often be in the form of optical signals, particularly for applications of interest to NASA, it seems worth while to inquire into methods for introducing this optical information into the guided-wave data-processing device directly—that is, without first converting the information to electrical signals or recording it on film or in some other way. This report presents the findings of such an inquiry as well as the results of some experimental work on a simple prototype device. In the following section, we describe the problem in more detail; discuss phenomena, materials, and device configurations; and assess the merits of various schemes. A section describing the experimental device and illustrating some more detailed design considerations follows. The final brief section contains a summary of the results and our conclusions.

SURVEY OF DEVICES, MATERIALS, AND PHENOMENA FOR DIRECT OPTICAL INPUT

Input-Optical Data Characterization

Without significant loss of generality we may assume that the optical information to be introduced into an optical waveguide and subsequently processed consists of a quasi-monochromatic beam, coherent or incoherent, with a one-dimensional spatial variation of intensity. This intensity distribution will also change with time; we shall assume that this temporal variation is in the form of regularly spaced pulses during each of which the spatial distribution is fixed. If the original information is not in this form, it may be possible to put it in this form by a suitable sampling procedure. To put it more explicitly, the input data will be characterized by

i) wavelength

ii) range of spatial frequencies present

iii) amplitude of spatial frequency variations

iv) dc background level

v) frame rate.

Some of these characteristics are indicated in Fig. 1. The materials and the device configuration of any direct-optical-input* device will obviously depend on these data characteristics and on the ways in which the data will be processed or used. As examples of types of uses to which the data may be put, we adduce the following:

i) determination of the presence or absence of certain spatial frequencies

* Henceforth abbreviated DOI.

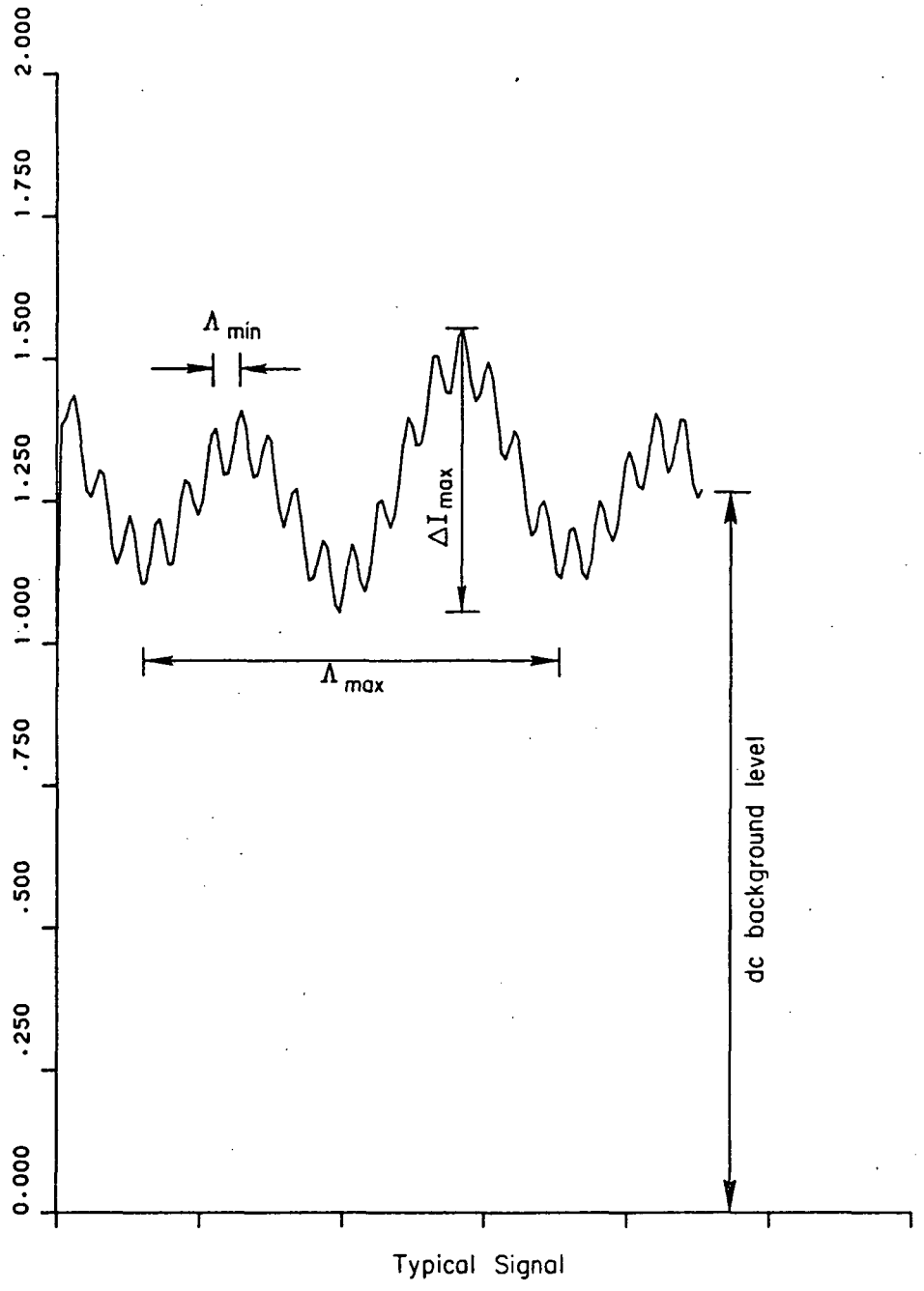

Figure 1. SKETCH OF LIGHT INTENSITY VS FUNCTION OF DISTANCE ACROSS BEAM FOR TYPICAL OPTICAL-SIGNAL ONE DIMENSIONAL INPUT DATA. ΔI_{max} = MAXIMUM LEVEL OF SIGNAL VARIATION. Λ_{min} = SHORTEST SPATIAL WAVELENGTH PRESENT, CORRESPONDING TO MAXIMUM SPATIAL FREQUENCY; Λ_{max} = LONGEST SPATIAL WAVELENGTH PRESENT, CORRESPONDING TO MINIMUM SPATIAL FREQUENCY.

ii) comparison with a reference signal

iii) correlation or convolution with another signal

iv) storage for future use.

Since there are both many sorts of input data and many ways to process them, we will not be able to provide a systematic survey of every case but will have to content ourselves with pointing out where some of the more attractive possibilities lie and what some of the tradeoffs are.

Types of DOI Devices

Even when the input data signal is specified, it will not be a simple task to enumerate the possible mechanisms and arrangements for transmitting the information on the signal to the guided beam. It will be helpful to categorize broadly the types of system components that may be encountered and the types of interactions that may be utilized.

We start with the guided beam. We may take it to be confined to a planar high-refractive-index layer at the surface of some optical material. The guiding layer may be homogeneous, as in many sputtered or epitaxially grown films, or it may be inhomogeneous, with the refractive index varying with depth, as in diffused or ion-exchanged guiding layers. This distinction will not generally be important for our purposes, except in the analysis of guided-mode-to-unguided-mode conversion, as discussed below. The guided beam may be extended, confined in only one dimension, as indicated in Fig. 2a, or it may be confined in two dimensions to a set of parallel channels (Fig. 2b) or ridges (Fig. 2c). Clearly, in the latter two types of waveguide structures, the range of spatial frequencies that can be detected will be limited by the channel spacing. (It will be convenient to refer to both these types of guides simply as channel guides.)

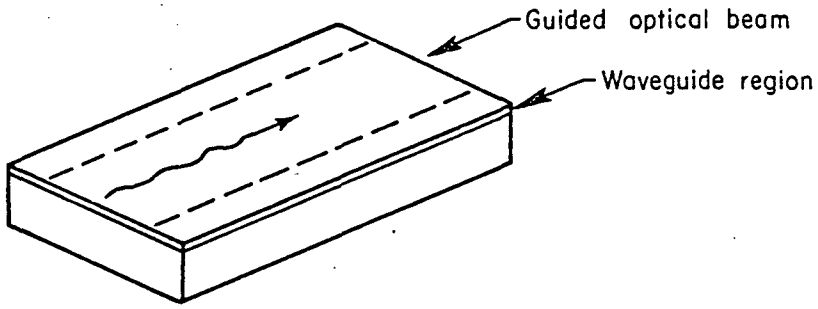

(a)

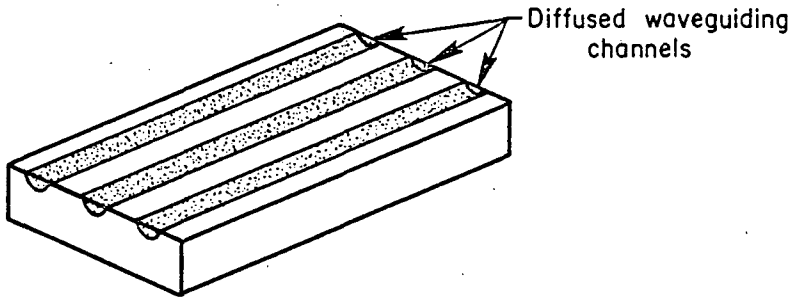

(b)

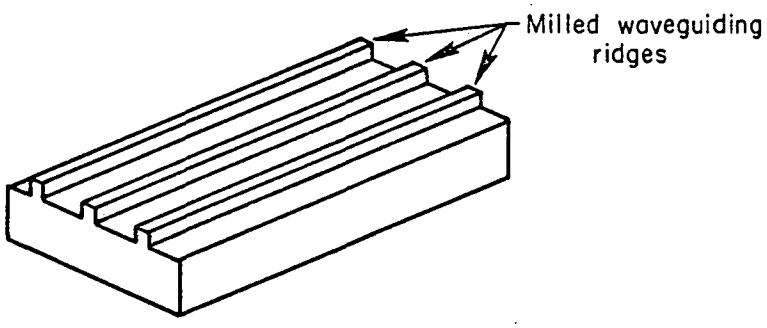

(c)

FIGURE 2. THREE TYPES OF OPTICAL WAVEGUIDES THAT MIGHT BE USED IN DOI DEVICES. MAGNIFIED SECTIONS OF A PORTION OF REGION ADDRESSED WITH A SIGNAL BEAM ARE ILLUSTRATED.

In any case, it is assumed that we deal with plane waves in an effectively isotropic medium. Effects of optical anisotropy in the guide, substrate, or overlays can be included if necessary, but it does not appear at present that any significant device concepts are overlooked by ignoring them. The number and polarization characteristics of the modes, at a given guided-beam frequency, supported by the guide will of course also be of prime importance.

The input information will be impressed on the beam in the form of a modulation of its amplitude or of its phase. The information may be analog—that is, the depth of modulation is proportional to (or at least a simple function of) the intensity level in a given channel or at a given position across the beam. Or the information may be binary, only the presence or absence of a signal above some background level in a given channel being impressed on the guided beam. There is also a possibility in some devices of introducing digital information other than binary, but we shall not explicitly discuss this case in the present report. Often we shall consider the simplest case of impressment of binary information in one channel of a channelized device. It will have to be borne in mind that successful operation of such a device does not necessarily guarantee successful operation of a corresponding analog device, say.

There are several locations where the signal beam may be detected and used to modulate the guided beam:

i) the interaction may take place in the waveguide itself if it is made of a suitable photosensitive material (Fig. 3a);

ii) the interaction may occur in a film or thick layer placed on the waveguide surface (Fig. 3b);

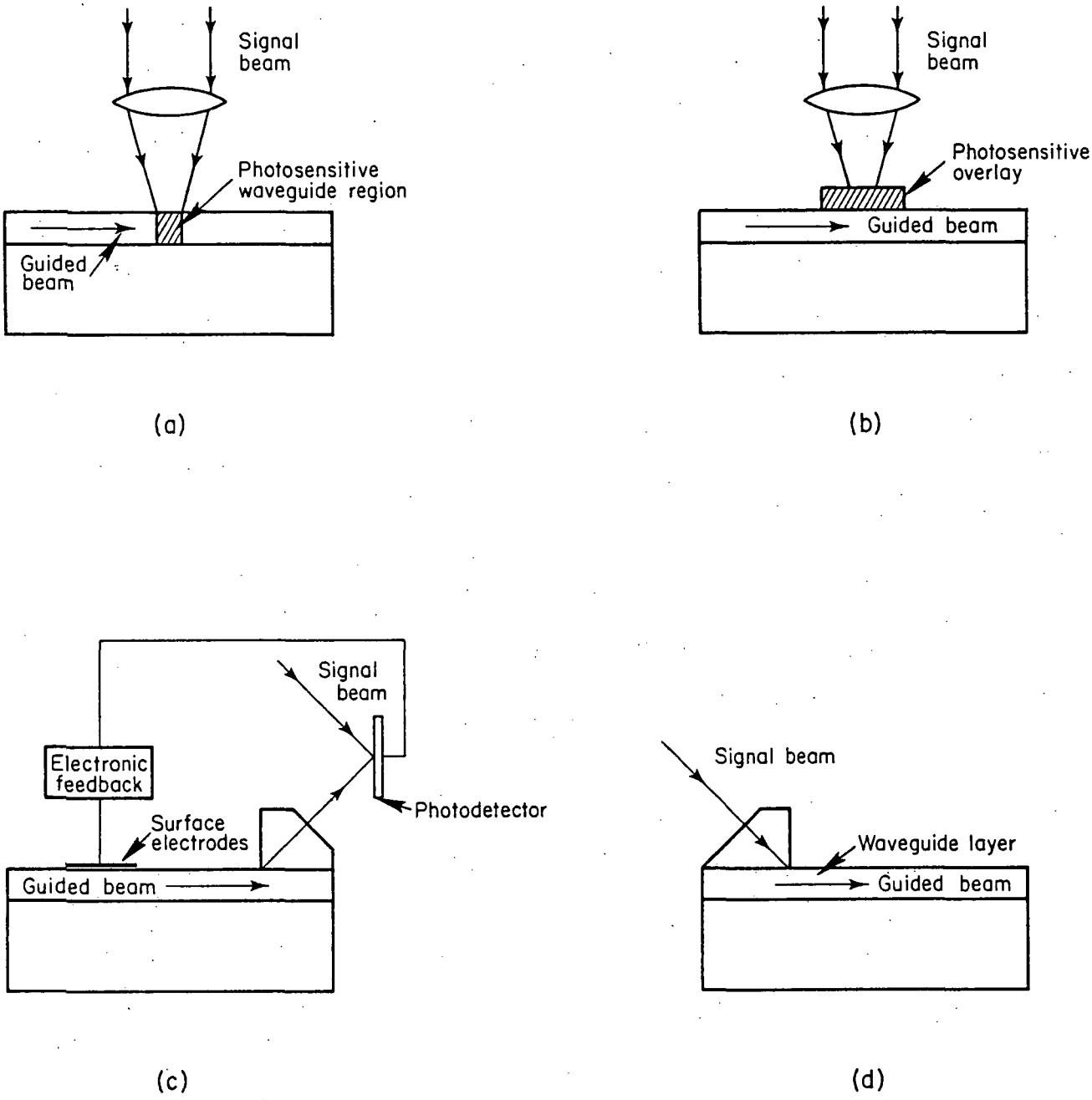

FIGURE 3. FOUR POSSIBLE CONFIGURATIONS FOR DOI DEVICES DIFFERING IN LOCATION OF PHOTOSENSITIVE LAYER.

iii) the signal beam may be detected by an external detector, perhaps on the surface of or in a different waveguide; this detector might (as in Fig. 3c) or might not also be intercepted by the guided beam or a portion of it; and

iv) in exceptional cases, the signal beam might simply be introduced into the waveguide and become the guided beam itself (Fig. 3d).

A few additional words need to be said about each of these configurations. In the first setup, the primary requirement is that the material be sensitive to the signal beam and insensitive to the guided beam; so the range of devices is somewhat limited. The second configuration is more versatile, since different combinations of materials may be used. It will often be the case that the photosensitive overlay material has a higher refractive index than the waveguide; so the guided beam will tend to run up into it. There are device configurations in which this may be exploited, but more often the overlay will be separated from the guide by a thin inert dielectric layer in order to keep the guided beam where it belongs. The third configuration is more versatile yet, since now the detection and modulation functions are physically separated, and intermediate electronic steps such as signal amplification are possible. Purists may with reason quibble about whether devices of this type truly represent "direct" optical input; however we consider any device that operates on a large number of parallel channels in real time as fair game. The fourth type of device is obviously the simplest; we mention it here mainly for completeness and will not discuss it in detail since it is not likely that the input data beam will be suitable for direct introduction in many cases.

The mention of external electronics suggests another way of classifying DOI devices:

i) completely passive

ii) electric fields applied

iii) optical signals amplified

iv) combination of ii) and iii).

Devices of the first type are possible in principle, but all those that we have been able to conceive require awkward thermal or optical cycles for erasure of induced signals; so in general we describe devices with electric fields. If amplification of optical signals is considered cricket, a wide class of multistable, feedback-controlled devices of types which have received a lot of attention recently[1,2,3,4] becomes possible. We shall not have a great deal to say about devices of this type inasmuch as the addition of amplification adds one more level of complexity to the devices. The present capabilities of devices of this sort are well described in the articles referred to and it is not difficult to see how the devices might be modified for direct optical input.

To complete the categorization of the possible device types, we need to specify

a) the physical mechanism by which the signal beam is detected,

and b) the way in which the guided beam is perturbed by the mechanism of a).

A wide variety of effects—photovoltaic, photoconductive, photochromic, photorefractive, thermooptic, etc.—may be exploited in detecting the the signal beam, and each of them occurs in a variety of materials. It

is not the place to describe them in detail here; they are more appropriately discussed in connection with specific devices in which they are used. Many of these effects are also of interest in connection with optical memory devices. This is a topic which has been repeatedly reviewed[5-8]. The information in these reviews is helpful in ascertaining the known capabilities of various materials and effects. Almost any type of integrated-optic modulator is adaptable to DOI. A recent review[9] lists six basic types, and several others are possible.

To recapitulate, a DOI device may be characterized by

1) Signal beam characteristics
2) Type of waveguide
3) Analog or digital operation
4) Physical configuration of signal-beam sensor relative to waveguide
5) Presence or absence of amplification
6) Signal-beam detection mechanism
7) Guided-beam modulation mechanism and modulator configuration.

This list clearly only provides a descriptive characterization; a functional or operational characterization—how and how well does the device work?—is equally necessary. Although we have not yet provided a descriptive characterization of a single device, it is to the question of functional characterization that we now turn. This is because enumeration of all the possible DOI devices would be a vast task, and functional characterization of even a moderately complicated one is a difficult problem involving optimization with respect to numerous design variables. What we propose to do, therefore, is to discuss

functional characterization for a limited class of very simple devices in order to indicate the capabilities of some of the phenomena of interest. Then we shall describe several more complex device configurations that seem to us promising, but whose operational characteristics can be only partially determined.

Materials/Phenomena Characterization of Simple Devices

We start with a simple single-channel phase modulator, such as is illustrated in Fig. 4a. Surface electrodes like those shown may be used to modulate the phase of the guided beam through the electrooptic effect in the waveguide material, and this modulation may be increased or decreased through the interaction of the signal beam with the waveguide material or with a suitable overlay (Fig. 4b). This is basically an analog device, but it can also be used as a binary switch. If the signal beam produces a change in the mode index of the guided beam of Δn and if the length of the interaction region along the guided beam is L, the change in phase shift will be

$$\Delta\phi = 2\pi\lambda_o^{-1}\,\Delta nL \quad , \tag{1}$$

where λ_o is the free-space wavelength of the guided beam. For most of the interactions of interest, it will be possible to write an approximate relationship of the form

$$\Delta n = \kappa\,\alpha\, I\tau = \kappa\,\alpha\, J\, W^{-1}\, L^{-1} \quad , \tag{2}$$

where κ is an empirical "constant", α is the absorption at the signal wavelength of the waveguide material, W is the channel width, τ is the recording

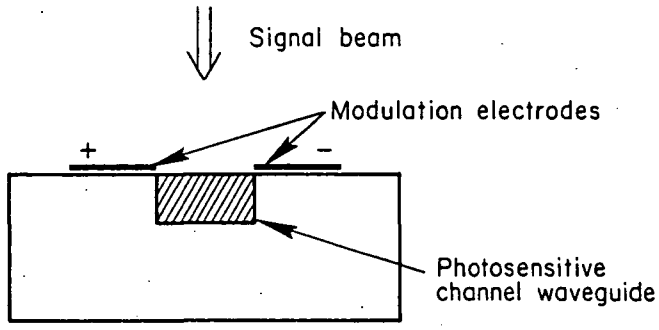

(a)

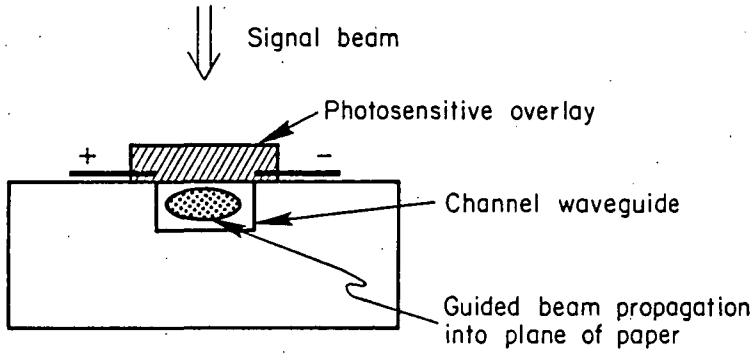

(b)

FIGURE 4. TWO CONFIGURATIONS FOR A SINGLE-CHANNEL MODULATOR.

time, and I is the intensity and J the total energy of the portion of the signal beam incident on the active region. Apparently

$$F = \lambda_o W(\Delta\phi) J^{-1} \tag{3}$$

would be a suitable figure of merit for comparing materials as phase modulators; however, it will be advantageous to express the comparison in terms of the signal beam energy necessary to produce a minimum reliably detectable phase shift, typically around 0.1 rad., for given values of λ_o and W. For the latter parameters we shall choose 0.8 μm and 5 μm respectively.

The only direct mechanisms for affecting the waveguide refractive index appear to be the photorefractive effect occurring in pyroelectric crystals and the photostructural photorefractive effect occurring in certain amorphous semiconductors. The photorefractive effect will not produce a completely uniform Δn across the channel, a complexity which we will ignore. The most sensitive known material for a photorefractive phase modulator[10] is $Bi_{12}SiO_{20}$. Optical waveguides have been made using this material, which has a relatively low refractive index compared to other sillenites[11], only by polishing samples until they are fairly thin.[12] Such guides support very many modes; still, because of its great sensitivity we shall consider this material for purposes of illustration. It is not pyroelectric, and is photorefractive only in the presence of a moderate electric field.* For a field of about 6 kV/cm, requiring around 5 V on our surface electrodes, and a signal beam wavelength of .51 μm, the product κα may be as small as 0.035 cm^2J^{-1}, meaning that an incident energy of around 2 pJ per channel will be sufficient

* In sufficiently strong fields, some other material, such as $KTa_{.65}Nb_{.35}O_3$, may be more sensitive.[13]

to produce a measurable phase change. For a channel 1 mm long and a recording time of 1 μs, an incident intensity change of about 0.04 W/cm^2 will be needed to produce this effect. An intensity of 1.1 W/cm^2 or total absorbed energy of about 60 pJ will produce the maximum detectable phase shift of π radians. To produce the π phase shift electrooptically with electrodes like those described would require roughly 10 nJ of capacitive energy, while obtaining 0.1 radian would take about 12 pJ. This material is comparable to photographic film in sensitivity; more familiar photorefractive materials such as iron-doped $LiNbO_3$ would require more than an order of magnitude more energy, and would not appear to be practicable. $Bi_{12}SiO_{20}$ crystals have point group 23 and thus display optical activity; we have assumed this phenomenon does not seriously degrade device performance inasmuch as does not seem to have been a problem in other work.[12] Another type of device using this material will be described later.

Semiconducting glasses such as As_3S_3 also appear to require somewhat higher recording energy[14] and they suffer from problems with incomplete erasure and high optical loss; so they seem more suitable at present for permanent surface gratings and similar structures than for DOI elements, either within waveguide layers or on their surfaces. We have not previously discussed cyclability and erasure as DOI materials parameters; we confine our remarks to a few generalities presented here:

i) any successful DOI material must obviously withstand many millions of record/erase cycles without fatigue;

ii) there are few known DOI phenomena which do not require some active erasure step; provision for this step will complicate the system optical and/or electronic design;

iii) the material properties controlling erasure and fatigue are generally different from those controlling writing sensitivity, yet similar in degree of difficulty in controlling or modifying. It will be best of course to try to design devices using materials for which erasure or fatigue are known not to be problems, but in view of the limited amount of study that has been given to these questions, this will not often be possible.

Devices with photosensitive overlayers (Fig. 4b) may be used in phase modulators in a variety of ways. By changing the overlay refractive index or absorption coefficient with the signal beam, for instance, the boundary conditions at the waveguide-overlay interface will be changed and this will change the mode index of the guided beam. This will be a small effect, though, better utilized in binary mode-conversion devices than in phase modulators. We should mention, however, that we have successfully demonstrated phase-modulation lenses working on very similar principles.[15] A less direct but more effective way to achieve phase modulation with an overlay material is to apply an electrooptic phase shift with the surface electrodes and then to reduce the electric field in the waveguide through shorting out the electrodes by illuminating a photoconducting overlay with the signal beam. We have conceived of several devices using this principle; some of them are described below. Perhaps the first device using a similar concept was constructed by Goldberg and Lee[16]. Dark/light potential ratios of 5 to 10, quite adequate to achieve measurable phase shifts, can readily be obtained with suitable load resistance and illumination. For fast commercial CdS cells, even with incandescent illumination, the optical switching energy to produce a dark/light resistance

ratio of up to 10^4 may be less than 1 $\mu J/cm^2$. With monochromatic illumination of the optimum wavelength, the energy sensitivity is probably comparable to the photorefractive devices discussed previously. Unfortunately, charge-trapping effects generally limit speed to the millisecond range, and fatigue effects may set in if too many switching cycles are attempted in a short time.

Another attractive concept is that of using a simple layer of black paint as the photosensitive overlay and producing the modulating electric field by the pyroelectric effect in a suitable crystal. Not enough information seems to be available to evaluate this idea quantitatively, but experiments[17] on $LiNbO_3$ indicate fields of suitable magnitude may be produced. Erasure occurs simply by the heated regions returning to ambient temperature; for fast cycle times some means of accelerating this thermal decay will probably have to be provided.

We may consider one-channel intensity modulators along the same lines as the phase modulators. We will consider analog modulators to start with; again the configuration may be that of Fig. 4a or that of Fig. 4b. The principal design problem in analog intensity modulators is that since there will ordinarily be a rather large signal propagating in the channel, it will be necessary to be able to detect reliably a small change in a large signal in order to achieve a large dynamic range. If a 0.1% change in intensity can be detected reliably over a long period of time—a detection sensitivity not trivially achieved—then a change of several percent must be obtainable upon illumination with the signal beam in order to produce a useful analog device. Suppose for purposes of analysis we consider a 1% intensity change. To produce this in a channel

of length 1 mm, such as we considered in the phase-modulator discussion, requires a change in absorption coefficient $\Delta\alpha$ of .05 cm^{-1}.

Let us consider first the possibility of optically altering the absorption of the waveguide material itself. By far the most sensitive of such photochromic processes are those involving optical reorientation of color centers[8] to produce, or to eliminate, dichroism. Although data useful for estimating recording sensitivity are hard to come by because of the inhomogeneous nature of the coloring process, the process appears to be comparably sensitive[7] to photorefractive recording in iron-doped $LiNbO_3$. The most suitable material for room temperature use, though, is NaF, which does not seem suitable for optical waveguides because of its very low index of refraction and ready solubility.

The most effective way to alter the attenuation using an overlay is with a photoinduced semiconductor-to-metal transition in the overlay material, since with a metallic overlay TM modes are strongly attenuated.[18] The only generally useful material for optically induced semiconductor-to-metal transitions appears to be VO_2, which will switch thermooptically[19] upon absorption of visible light heating a film of the material to its transition temperature of 68°C. This material has a large positive real part of the dielectric constant in both phases throughout the visible, though; this means that it will tend to suck the guided beam into it, or will strongly modify the propagation in the guide if the VO_2 film is too thin to support a guided mode on its own. Thus to keep the guided mode from switching the film itself, it will have to have an energy well below the bandgap of 0.8 eV, i.e., a (free-space) wavelength longer than 1.6 μm. It is difficult to see how this effect could be used to impress analog

information on the guided beam since the film switches or it doesn't; inasmuch as the attenuation can be quite substantial, a binary device might be possible. To switch a 0.8 μm film on a channel 1 mm long and 5 μm wide requires around 1.5 μJ of signal beam energy.[19] The energy density required for switching depends strongly on the quality of film preparation. Switching speeds in the microsecond range are possible.

As a final type of simple device, we wish to discuss a guided-to-unguided mode converter. This is a binary device; typically, when the signal beam is on, the effective index of the guided beam is reduced to the extent that the beam is no longer guided and escapes into the substrate. Since the guided beam is what is usually detected, this device also performs the logical operation of negation. Again either the arrangement of Fig. 4a or that of Fig. 4b may be considered. Since only a small change in refractive index may be required to "unguide" the beam, devices of this type can in principle be very sensitive. Just how close to cutoff one can propagate, though, depends primarily on the ability to prepare reproducibly uniform waveguide layers of prescribed index profile. It might sometimes be possible, though, to rescue beams that aren't quite guided by applying a small potential to the electrodes to produce an electro-optic Δn. Also, the mode index is not the only factor to be considered; the index profile will also be important. For example, in a single-mode out-diffused $LiNbO_3$ waveguide, the effective index of the guided mode may be only around 10^{-4} greater than the substrate index,[20] but the effective waveguide thickness will be several tens of microns and it may be more difficult to get a beam to go from guided to unguided by a change in surface boundary conditions than it would be in a shallower waveguide with a higher

mode index. On the other hand, if the waveguide itself is sensitive to the signal beam, photorefractive changes like those discussed previously can easily simply wipe out the guide over a sizable distance.

It is of more interest to inquire whether, with this apparently very sensitive arrangement, we can push a mode beyond cutoff with a modest photoinduced change in the overlay refractive index. Quantitative estimates can be made by using the WKB approximation to determine the effective mode refractive index as described by Hocker[21]. If we adopt the approximation, widely used in discussion of overlay effects, of an exponential dependence of diffused-waveguide refractive index on distance from the surface; and if we ignore relatively small effects due to guiding in a channel rather than with an extended beam, a fairly simple explicit expression for the overlay index change can be found.* We will also assume that the overlay refractive index is less than that of the wave; this means that tolerance requirements on the thickness of the overlay may be eliminated from consideration. To explain the calculations, we have to introduce some terminology and notation. Let

n_b = bulk refractive index of waveguide material

n_a = refractive index in dark of overlay

n_{eff} = effective index of waveguide mode

n_o = refractive index at surface of waveguide

ε = change in overlay index sufficient to cut off lowest-order mode

* A similar explict expression could be obtained for a homogeneous waveguide, but we have not considered worthwile to evaluate this, since inhomogeneous guides should be easier to cut off because the optical energy in them tends to travel in a submerged layer, more away from the surface.

$$\delta = n_{eff} - n_b$$

$$\Delta = n_o - n_b$$

Then we can define a normalized mode index b by

$$b = \delta/\Delta \tag{4}$$

for modes near cutoff. Following Hocker, we also define an asymmetry parameter a, for the overlay unilluminated, by

$$a_{TE} = (n_b^2 - n_a^2)/2\, n_b \qquad \text{for TE modes} \tag{5a}$$

and

$$a_{TM} = (n_o/n_a)^4\, a_{TE} \qquad \text{for TM modes.} \tag{5b}$$

Now we let α be the change in the parameter a necessary to cut off the lowest-order mode. It is straightforward to show that α is related to the overlay index change ε by

$$\alpha_{TE} = -(\varepsilon/\Delta)(n_a/n_b) \qquad \text{for TE modes} \tag{6a}$$

$$\alpha_{TM} = -(\varepsilon/\Delta)\,(n_b/n_a)^4\,(1 + 4\Delta n_b^{-1})(2n_b^2 - n_a^2)/(n_b n_a) \qquad \text{for TM modes.} \tag{6b}$$

As we might expect, a decrease in the overlay index is needed to cut off the mode. With these definitions in hand, we can show that for <u>either</u> polarization of the guided mode we can find the value of α, given a and b, from

$$(\pi/4 + \tan^{-1}(a+\alpha)^{1/2})((1-b)^{1/2}b^{1/2}\tan^{-1}(1-b)^{1/2})$$

$$= \pi/4 + \tan^{-1}((b+a)/(1-b))^{1/2}\ , \tag{7}$$

where we have used the fact that, just at cutoff, b = 0. This expression is easy enough to evaluate, but because of the large number of parameters, it is not easy to see how the effects vary with changes in the parameters except by considering specific examples. One generalization that can be drawn from calculations of the solutions of (7) is that small values of a correspond to high sensitivity of the mode index to changes in the overlay index. However, since the obtainable range of Δ is rather limited, small a corresponds to n_a quite close to n_b, and we may have practical difficulties keeping the guided beam in the original waveguide layer. Also, for TM modes, we can see from Eq. (5b) that very small values of a_{TM} correspond to values of n_a higher than n_b. For purposes of illustration, let us consider a Ni-indiffused waveguide* in $LiNbO_3$ with a guided beam of wavelength of 0.6328 μm. Then, typically,

$$n_b = 2.20 \quad \text{for TE modes,}$$

$$n_b = 2.29 \quad \text{for TM modes,}$$

$$\Delta = 10^{-2}.$$

For the overlay, let us assume $a = 1.0$. Then

$$n_a = 2.190 \text{ for TE,}$$

$$n_a = 2.281 \text{ for TM.}$$

This situation might in principle be achieved by growing epitaxially a $LiNbO_3$ film of slightly different stoichiometry on the waveguide. The overlay film would also be doped, say with iron, to make it sensitive to

* Ni waveguides in $LiNbO_3$ are reported to be relatively free from photorefractive effects.

the signal beam. Then if b = 0.1, so the guided beam has an index within 0.001 of cutoff, we find from (7) that $\alpha = 209$. For TE modes Eq. (6a) shows that this corresponds to a required change in overlay index, ε, of -2.1! If b = 0.01, not too easy to achieve, then $\alpha = 0.825$, corresponding to an overlay index change of $\varepsilon = -0.0083$ for TE modes and $\varepsilon = -0.0079$ for TM modes. These are large index changes to obtain photorefractively, but they might possibly be obtained in some other way. For smaller values of Δ, such as might correspond to outdiffused guides, similar calculations indicate that the hypothesis advanced above is correct—that is, such modes will actually be more difficult to cut off unless the waveguide quality is remarkably high. Of course we should properly take into account differences in the index profiles between outdiffused and indiffused guides in making this comparison, but we do not believe the qualitative conclusions will be altered. All in all, changing mode cutoff conditions by photoinduced changes in the overlay index does not appear to be an easy way to put optical information on a guided beam, although there might be some circumstances where it would work.

To summarize this discussion of several simple methods for DOI in a single channel, all may work in principle, but most require rather special materials and waveguide configurations. The most immediately applicable idea, not requiring extensive materials development work, is the photoconductive overlay. It is limited in speed, though.

Description of Some More Complex Devices

We now proceed to discuss a number of more complex device designs. Because of their greater complexity, it has not been possible to make

materials sensitivity calculations like those in the preceding paragraphs. Some quantitative results concerning the operation of several of the devices are presented, however. These ideas are not presented in any particular order.

A. Guided-Unguided Mode Conversion with Photoconducting Substrate

This is an adaptation of the Itek PROM device[22] in which electrooptic properties of a material are affected by charge trapped at an insulator-photoconductor interface. A sketch of the proposed setup is shown in Fig. 5. The bias field through the substrate causes charge to accumulate at the waveguide upper surface wherever the signal beam impinges. This affects the waveguide Δn electrooptically, leading to loss of guiding. As with the photorefractive effect, one of the most sensitive materials is $Bi_{12}SiO_{20}$, in a suitable external electric field. It may be possible to deposit a very thin (1-2 μm) waveguiding layer of another sillenite, such as bismuth gallate, $Bi_{24}Ga_2O_{39}$, on bismuth silicate by liquid phase epitaxy[23] or by sputtering.[12] This layer should, like the substrate, be strongly electrooptic and photoconductive in the blue. Thus as in the Itek PROM the device would use blue light to write and red light (TE mode) to read. A coherent write beam is not required. In some ways this is simpler than the PROM; a dichroic mirror is not needed, and only one surface needs good optical finish. There are some possible disadvantages, as well. For one thing, periodic exposure to a uniform erase beam is necessary. Primarily because of the erasing step, commercial PROM devices are limited to about 30 frames/sec, too slow for 1-dimensional data such as would be processed with the integrated system discussed here. An improved repetition rate with modified system design is probable, but it is unlikely any photoconductive system will ever be really fast as we have mentioned before. Another possible difficulty is that the materials involved are

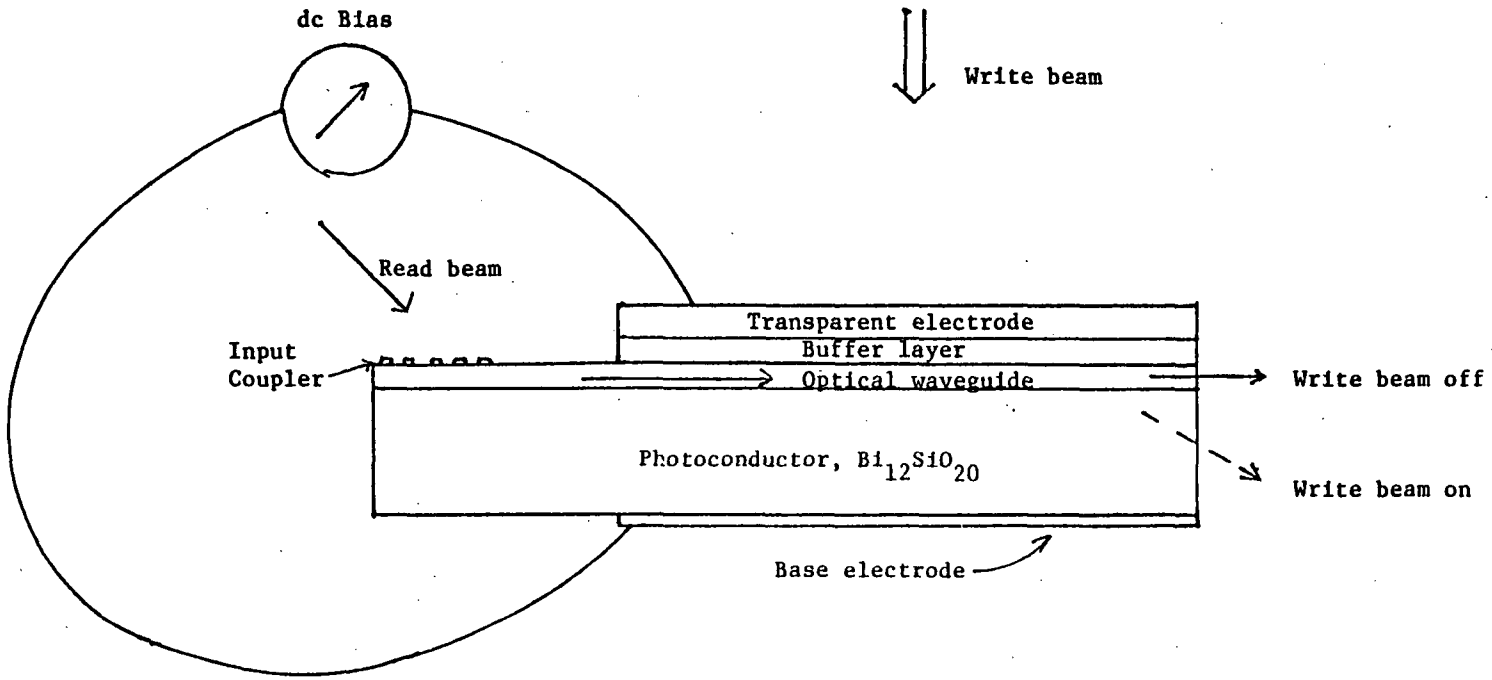

Figure 5. Schematic cross-section of PROM-type device for putting optical information on guided optical beam. Not to scale.
The write beam liberates charge carriers which are trapped at the buffer-waveguide interface. This produces an internal field which affects the waveguide refractive index through the Pockels electrooptic effect.

optically active; so the propagating modes are not truly TE or TM. The fact that one can write only with blue or uv light reduces the number of possible applications; all photoconductive devices will have some similar signal-beam wavelength restrictions of course.

A very similar device was recently described and demonstrated by Hayashi and Fujii.[12] The only substantial differences are that instead of a separate waveguiding layer, they simply used a thin $Bi_{12}SiO_{20}$ crystal slab as the waveguide; and they used an external polarizer and analyzer to permit analysis of phase information. The optical activity of the crystal did not prevent obtaining excellent extinction of the guided beam. Both transient and persistent optical impression of information on the guided beam, using the electrooptic and photoconductive properties of the material, were demonstrated.

B. Direct Optical Address Based on Total Internal Reflection

Figure 6 shows a waveguide switch based on total internal reflection. It consists of a V-electrode that surrounds a ground electrode parallel to one side of the V. The region between the parallel electrode segments has been treated so that its refractive index is less than that of its surrounding. The apex angle of the V is chosen so that an incident horizontal beam will be totally reflected when it encounters this region.

When a voltage is applied to the V-electrode, an electrooptically induced prism is established that results in a slight bending of the incident beam. The bending is in the direction required to frustrate total internal reflection (TIR). At the same time, the electric fields in the region of lower refractive index cause an increase in that refractive index. This

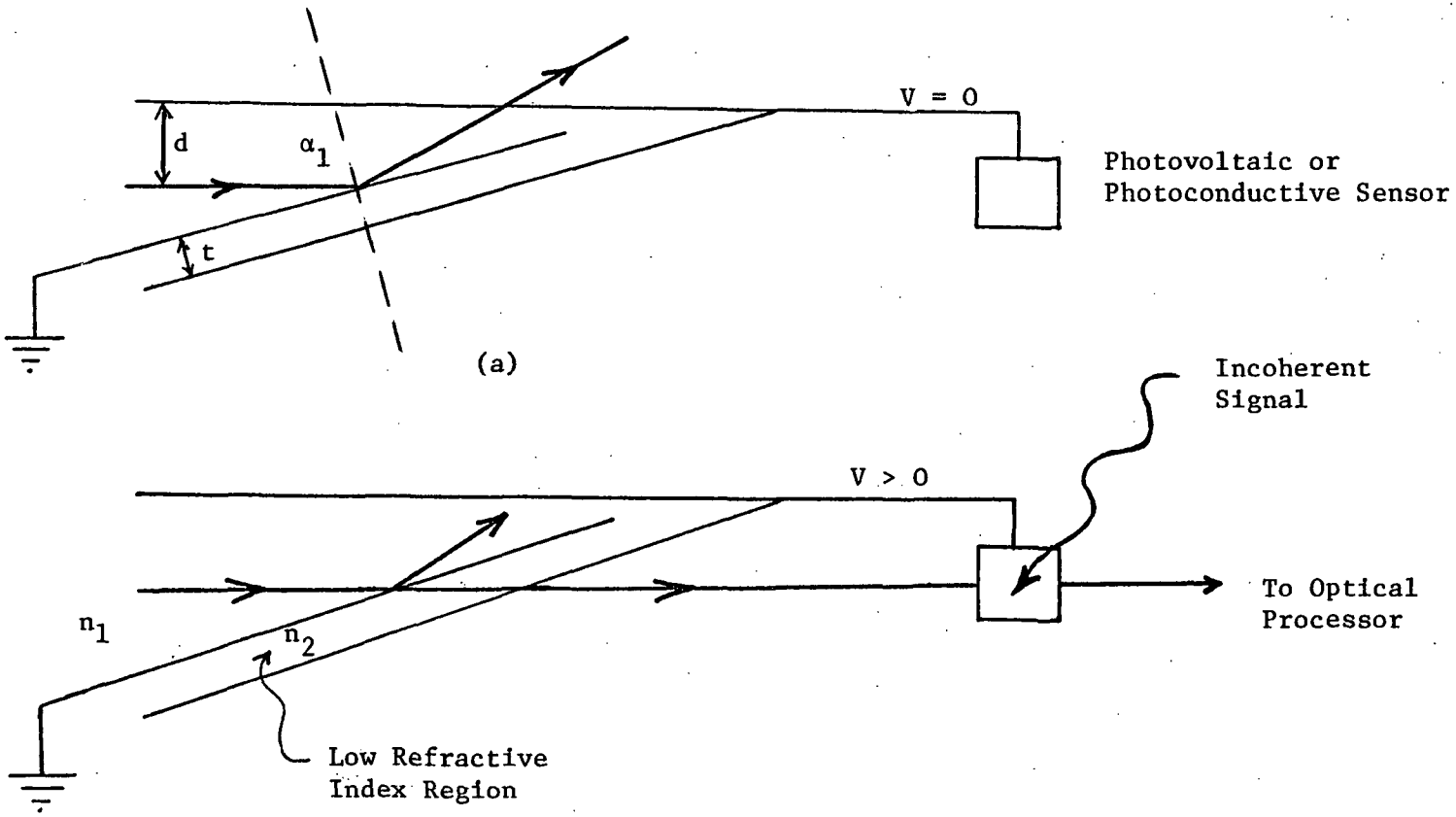

Figure 6. A Switch for Direct Optical Address Based on Total Internal Reflection at a Boundary of Reduced Refractive Index. (a) off state; (b) on state.

enhances the extent to which total reflection is frustrated. As a net result, light is transmitted through the switch. This light is caused to pass beneath a voltage-generating device,* where energy in the evanescent tail (or in the guided beam, if the refractive index of the voltage-generating element is high) is absorbed to produce an increase in voltage above that which was used to initiate the switching action. The process continues until a steady state is established. Light transmitted beneath or through the voltage generator is available for coherent optical processing.

The essential idea of this device is the separation of the information-recording and guided-beam-direction processes using the low-voltage small-angle electrooptic switch. This device thus falls in the category illustrated in Fig. 3c. The incoherent illumination of interest is imaged onto a device capable of producing a voltage monotonically increasing with the incident intensity. In the device, as described so far, the voltage signal perturbs the guided beam in such a way that part of the guided beam is redirected toward the voltage generator, thus producing an increase in voltage. This feedback enhances the perturbation of the guided beam so that a large effect may be attained for a small incoherent signal. The extreme nonlinearity possible in this type of device may be advantageous in certain applications, such as gray-scale slicing. However, configurations that can be employed without feedback are also feasible if the incoherent illumination is sufficiently strong. In this case, system response is linear if the photoelement response is, and therefore the output information could be used as the input to a multichannel data

* This element could be photovoltaic cell or a photoconductor in series with an external dc voltage source.

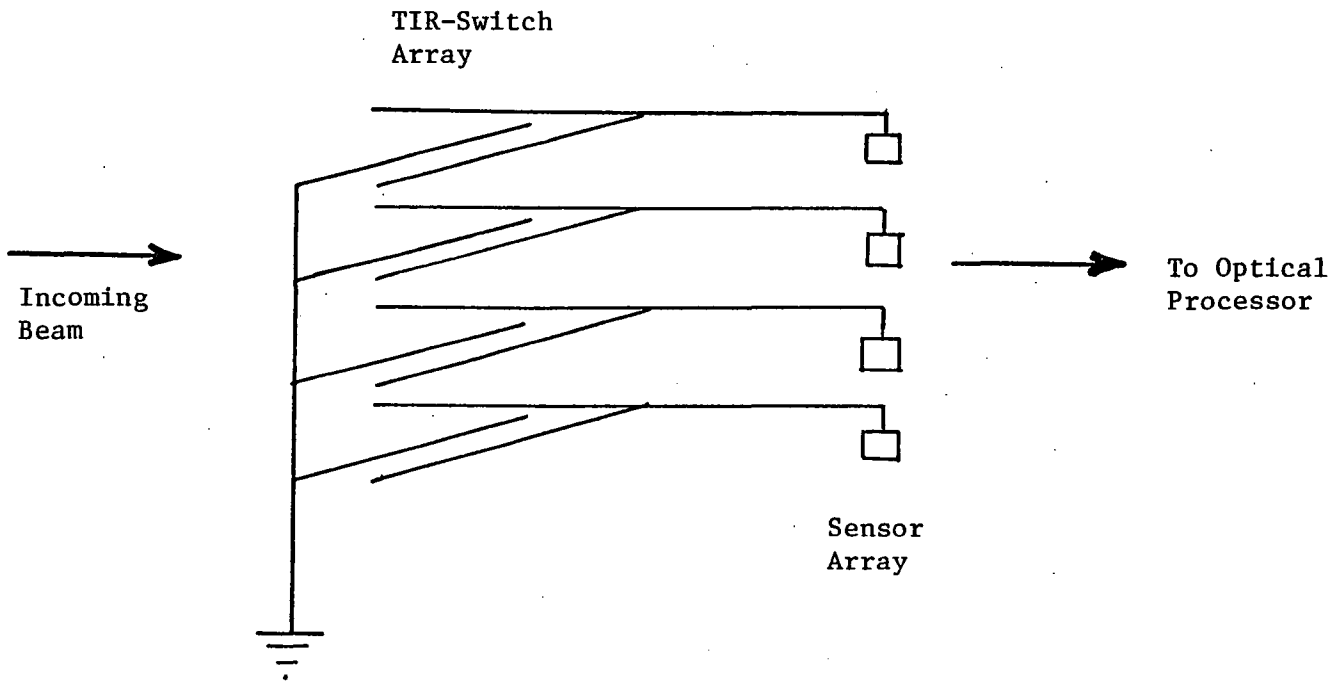

Figure 7. An Array of TIR Switches for Providing Four Channels of Coherent Optical Information. Incoherent Optical Information is Imaged on the Sensor Array.

preprocessor, for example. When feedback is used, the output discriminates sharply between "off" and "on" states. The switch described here is a modification and generalization of those discussed by Naitoh et al[24] and by Sheem and Tsai.[25]

Figure 7 shows how these switches could be operated in a parallel array. The output from each switch provides an optical information channel.

An analysis to determine the range of operating voltages and some other parameters of a practical device is not difficult. We suppose, for definiteness, that the device is built on a Y-cut $LiNbO_3$ crystal with a titanium in-diffused waveguide, and that the beam initially propagates perpendicular to the c-axis. For a TE mode, Fresnel's laws give for the reflectivity at the interface between the regions with refractive indices n_1 and n_2

$$R = \left(\frac{n_1 \cos \alpha_2 - n_2 \cos \alpha_1}{n_1 \cos \alpha_2 + n_2 \cos \alpha_1}\right)^2 \qquad (8)$$

where α_1 is the angle of incidence (Fig. 7a) and α_2 is the angle of refraction, related to α_1 by Snell's law

$$n_1 \sin \alpha_1 = n_2 \sin \alpha_2 \quad . \qquad (9)$$

The index difference $\Delta n = n_1 - n_2$ that can be readily obtained in $LiNbO_3$[24] is around 0.0026, a 0.12% reduction, according to Naitoh and coworkers. For this Δn, $\alpha_1 = 87.21°$. When a voltage is applied to the electrodes, n_2, α_1, and α_2 in Eqs. (8) and (9) must be replaced by n_2', α_1', and α_2', where

$$n_2' = n_2 + \frac{n_1^3 rV}{2t} \quad , \text{ and} \tag{10}$$

$$\alpha_1' = \alpha_1 - \zeta, \quad \text{where}^{(2)} \tag{11}$$

$$\tan \zeta = \frac{n_1^2 rV \sin^2 \alpha_1}{d(\pi - 2\alpha_1)} \tag{12}$$

In these equations, V is the voltage applied,* r is the appropriate electrooptic coeffiicient (r_{33}, with a value of about 30 x 10^{-12} m/V, for the geometry discussed here), t is the thickness of the reduced-index region, and d is the offset of the further edge of the incident beam from the upper electrode. (The dimensions t and d are shown in Fig. 6). In deriving Eq. (12), it is assumed that

i) the electrodes are long compared to d, and

ii) the overall index changes in the prism region have negligible effect compared to the beam-deflecting effects of the index gradients. The validity of the former assumption may easily be ensured experimentally—electrodes 2 or 3 mm in length should be adequate—while the latter assumption will only cause us to overestimate slightly the required switching voltages.

As lower limits to the structural dimensions that might be used, we chose t = 10 μm and d = 25 μm. The reflectivity at the interface was then calculated using Eqs. (8)-(12) and the other parameters given previously. The results of this calculation are shown in Fig. 8. While most of the

*Strictly speaking, the voltage applied to the beam. The voltage applied to the electrodes will have to be slightly larger because of fringing field effects.

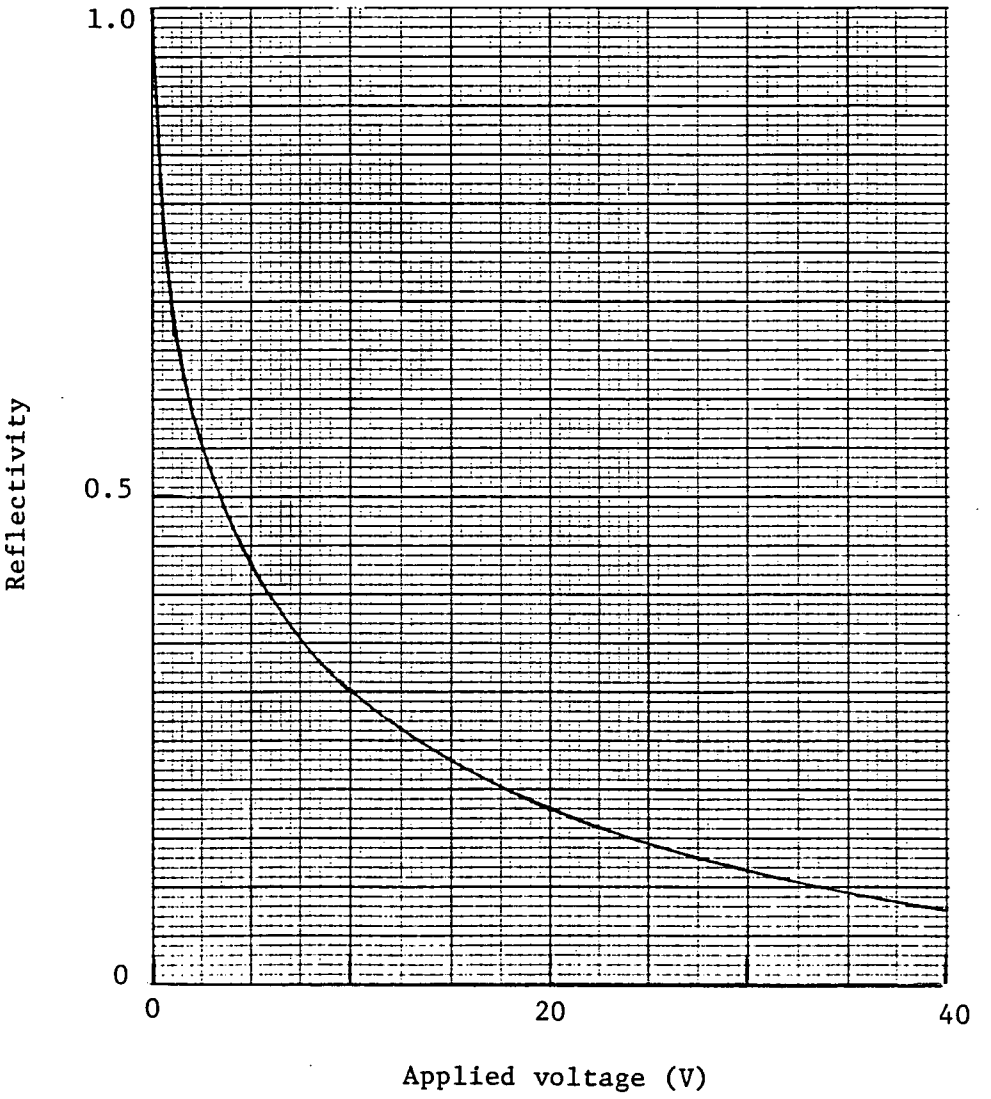

Figure 8. Calculated Reduction in Reflectivity of Total-Internal-Reflection Switch on $LiNbO_3$ When Voltage is Applied to Electrodes.

assumptions are "optimistic" in the sense that they tend to reduce the calculated switching voltage, it appears that useful switching might be accomplished at voltages not exceeding 10 V. The electrooptic prism effect reduces the switching voltages in the present device considerably from those that would be needed with the parallel electrodes alone.

Two points not considered in the calculations should be mentioned:

1) a beam incident just at the critical angle will leak through the low-index barrier region no matter how thick it is. To prevent significant leakage, the incidence angle should be increased a few hundredths of a degree.

2) the narrow (10-15 μm diameter) incident beam will tend to have a considerable diffraction spread. Means will have to be provided to reduce this over a considerable depth of field (close to 200 μm) if intolerable off-state transmission is to be avoided.

A single simple photovoltaic device such as a solar cell cannot provide the open-circuit voltage required to operate these switches. Among the ways sufficient switching voltage might be provided are

1) use of several cells in series, such as in the miniature solar-cell array used by Smith el al[4]

2) use of a high-voltage photovoltaic effect,[26,27]

3) use of switch capable of operating at lower voltages (around 1 V). As lower voltage switches, integrated Mach-Zehnder interferometers[28,29] and integrated stepped $\Delta\beta$-reversal switches[2] might be considered.

Devices of this type offer in principle several advantages, including

1) great design flexibility,

2) low required signal intensity, and

3) provision for latching or bistable operation.

C. Direct Optical Address Based on the Angular Selectivity of Bragg Gratings

Figure 9 shows an alternative type of switch based on the angular selectivity of Bragg gratings.[30] In this case, an N-electrode structure[31,32] is used to accomplish a slight voltage-dependent bending of an incident beam. The components are aligned so that when no voltage is applied, the incident beam passes through the grating without being diffracted. As a voltage is generated by an incoherent signal of interest, the guided beam is bent toward the direction of Bragg incidence. This results in a diffracted signal which, if desired, may illuminate the voltage generator to accomplish feedback. Fig. 10 shows how a number of Bragg switches may be operated in a parallel array. The diffracted output from each Bragg switch is used for coherent processing after passing beneath the voltage generator.

Twenty volts applied to the N-electrodes are required to go from minimum to maximum diffraction efficiency, assuming 1-mm long electrodes with a 100-μm aperture, for an aspect ratio of 10. The required switching voltage varies inversely with the aspect ratio; several volts should be sufficient for a useful device. Further enhancement of sensitivity could result from optimizing the N-electrode design. It seems likely that this design will require lower voltages than the TIR switch design; however it may require more space.

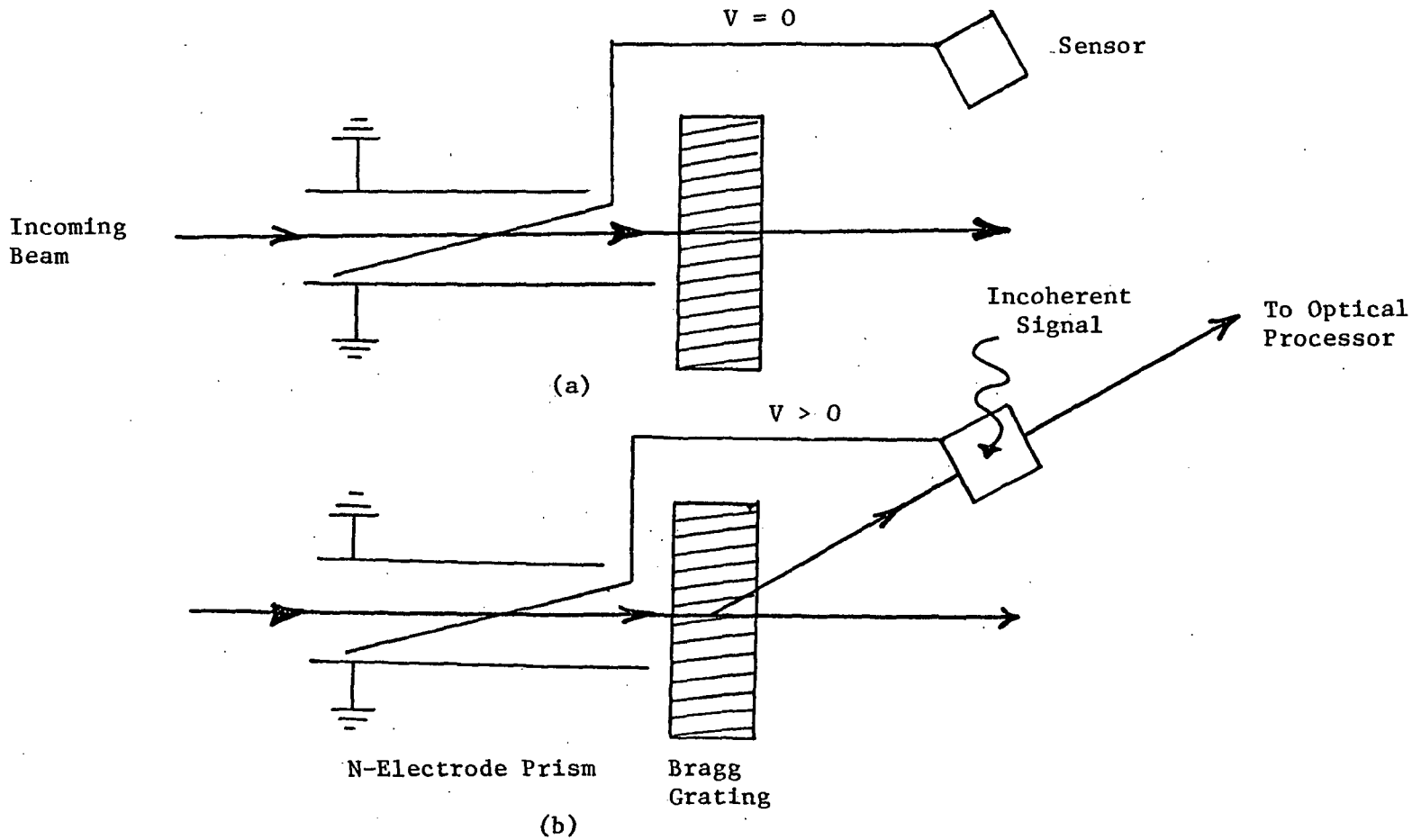

Figure 9. A Switch for Direct Optical Address Based on the Angular Selectivity of Bragg Gratings. (a) off state; (b) on state.

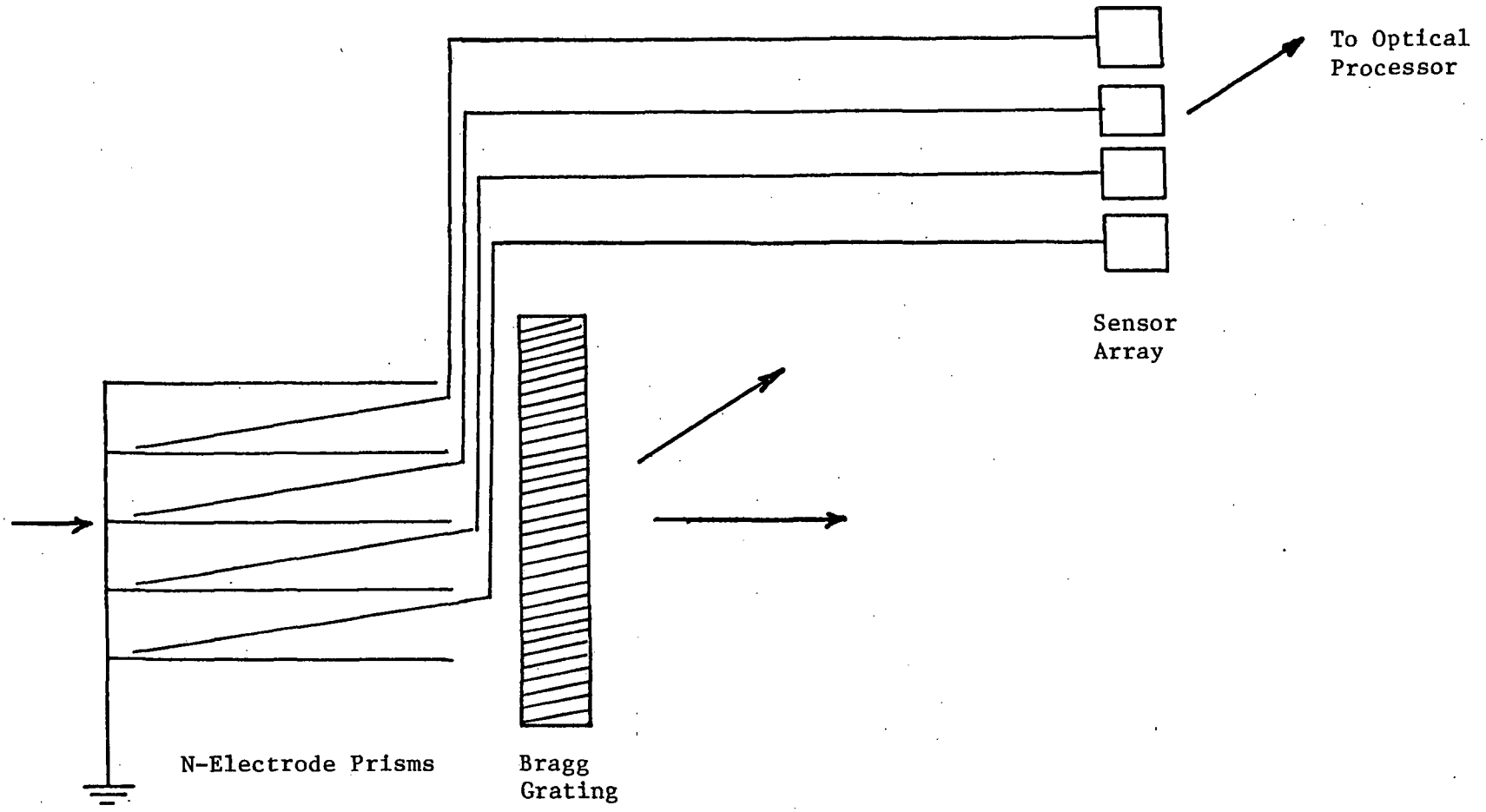

Figure 10. An Array of Bragg Grating Switches for Providing Four Channels of Coherent Optical Information. Incoherent Optical Information is Imaged on the Sensor Array.

D. Dual-Waveguide Phase Modulator

Many of the materials compatibility and guided beam-photosensor interaction problems encountered can be alleviated by pushing further the idea of photoelements that may be separated from the waveguide which has been mentioned in connection with the foregoing concepts. Just as an example of this, we show in Fig. 11 one channel of a device involving two separate waveguides. This device combines elements of the Fig. 3c and Fig. 3d arrangements. The signal beam propagates in the inexpensive glass waveguide; and is intentionally drawn up into the high-refractive-index photoconductor, increasing the voltage on the signal electrodes and thus phase-modulating the response beam.

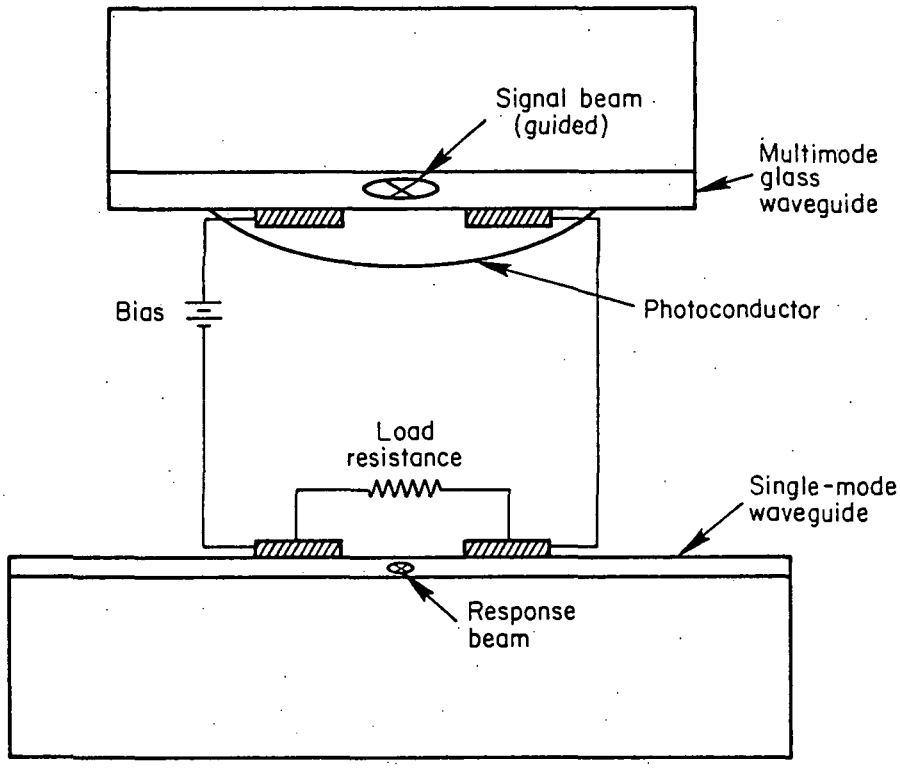

FIGURE 11. SCHEMATIC DIAGRAM OF ONE-CHANNEL OF A DUAL-WAVEGUIDE DOI PHASE MODULATOR.

A SIMPLE EXPERIMENTAL DEVICE

In order to study more thoroughly the factors involved in detailed device design and optimization, and to demonstrate that workable DOI devices can at least be constructed in the laboratory, we undertook the assembly and analysis of a simple experimental device. This device is basically a photoconductive-overlay phase modulator of the type previously described, with the phase modulation being converted to amplitude modulation by phase-modulating adjacent pairs of channels oppositely with the signal beam and causing the output beams from these channels to intersect and interfere by using a lens. A sketch of the experimental arrangement is shown in Fig. 12. The waveguide layer, made by outdiffusion on $LiNbO_3$, supported two TE modes. An inexpensive CdS photocell, with an irregularly interdigitated electrode pattern as indicated in the figure, was clamped face-down on the waveguide in such a way that the guided beam passed beneath two parallel adjacent unelectroded strips of photoconductor, also as indicated in the figure. These unelectroded regions are about 5-6 mm long and about 0.6 mm wide. The fingers of the electrodes are about 0.2 mm wide. The photocell has a plastic coating; because of this, the electrodes are about 7-8 μm above the surface of the waveguide. The dark resistance of the photocell is greater than 10 MΩ; this drops to 10-20 kΩ under strong illumination.

When a voltage in the range 100-300 V is applied to the electrodes, an interference pattern with two peaks appears in the focal plane. Upon illumination of the photocell through the $LiNbO_3$ crystal with the incoherent signal beam, the interference pattern collapses to the central focal spot. The switching time for this effect was not measured, but was too short to

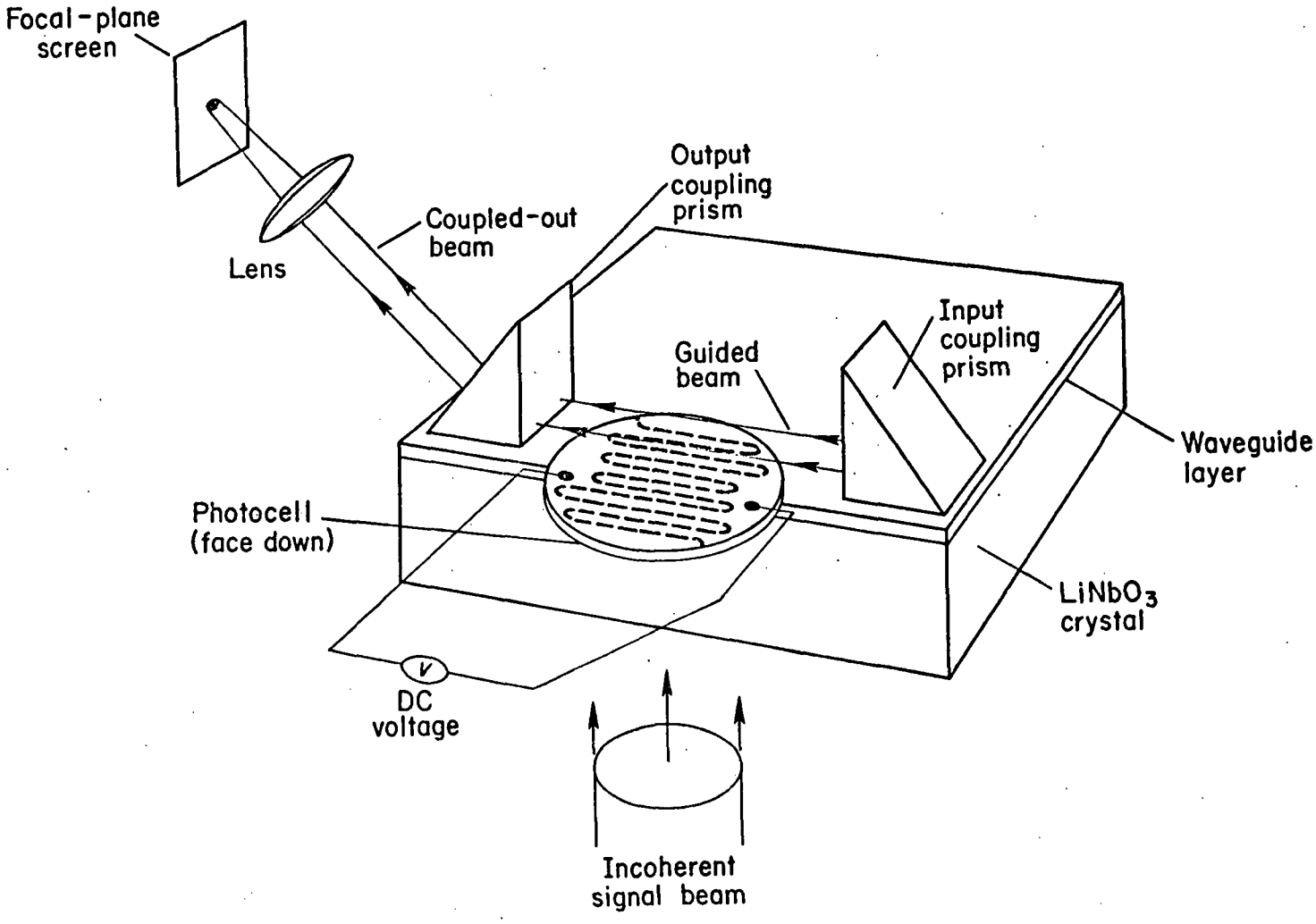

FIGURE 12. SCHEMATIC DIAGRAM, NOT TO SCALE, OF EXPERIMENTAL ARRANGEMENT FOR DIRECT OPTICAL INPUT EXPERIMENT USING PHOTOCONDUCTIVE CELL. DOTTED LINE ON PHOTOCELL REPRESENTS UNELECTRODED REGION.

discern by eye. A detector or data-processing element with its input at the center of the focal spot will respond strongly when the signal beam is on. There are several ways such a device might be further miniaturized and integrated to provide part of a compact data-processing system. We have described and demonstrated an "on-off" device, but devices are also feasible in which the recorded light signal is proportional to the input light intensity.

The operation of the device may be explained as follows. Applying voltage to the photocell causes electric fields in the waveguide region as shown in Fig. 13(a). Through the Pockels electrooptic effect, these fields alter the effective refractive index of the beam in the regions where they exist. Since the Pockels effect is linear in the electric field, the field-induced refractive index change δn will be of one sign in the region between the left and center electrodes and of the same magnitude but the opposite sign in the region between the center and right electrodes. To the simplest approximation, ignoring all fringing field effects, the situation is as indicated in Fig. 13(b). Thus the portions of the guided beams propagating in the regions marked "i" and "ii" in Fig. 13(b) will emerge from the electrode region with phase shifts, relative to the beam propagating under the electrode in region iii, given by

$$\eta = \frac{2\pi}{\lambda_o} (\delta n L) \quad , \tag{13}$$

where λ_o is the free-space wavelength of the guided beam (0.6328 μm in our experiments) and L is the electrode length. We can determine the expected effect of these phase shifts on the intensity distribution in the focal plane of the lens by using the formulas for the Fourier-transforming property

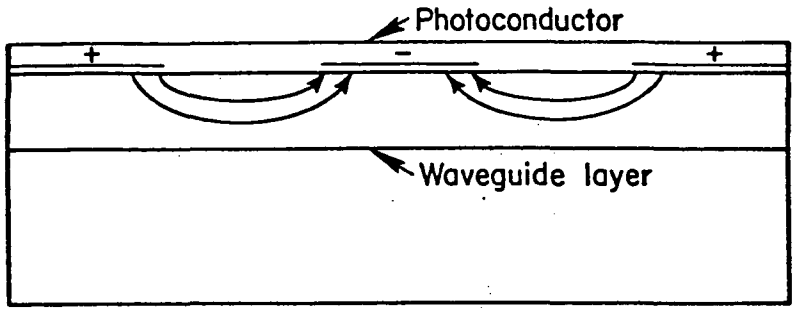

(a)

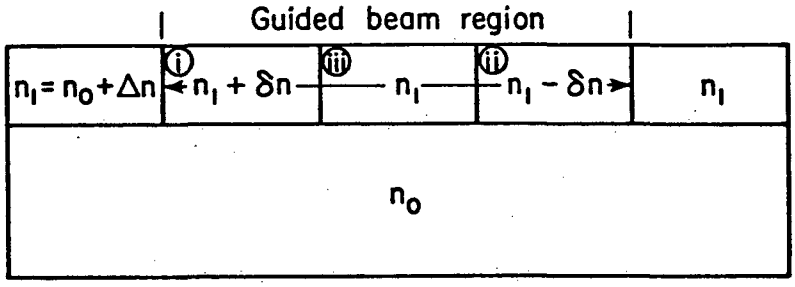

(b)

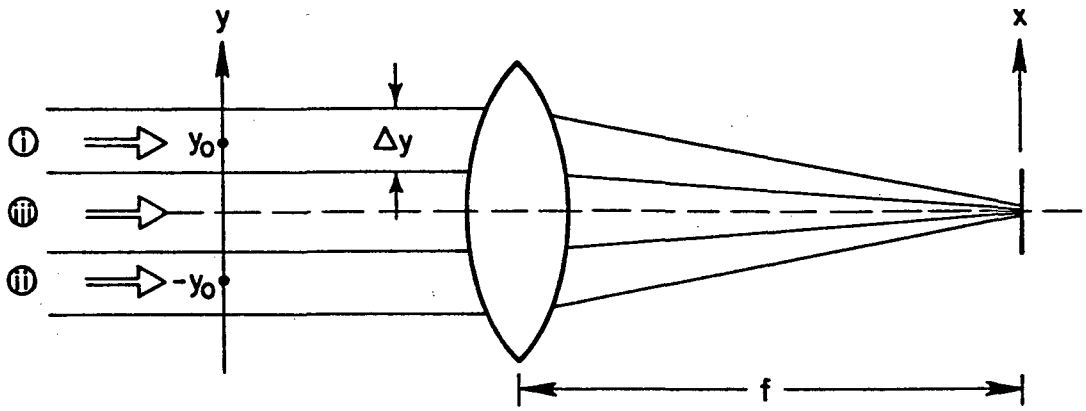

(c)

FIGURE 13. OPERATION OF DEVICE OF FIGURE 12. (a) ELECTRIC FIELD PRODUCED IN WAVEGUIDE REGION BY SURFACE ELECTRODES. (b) APPROXIMATE REFRACTIVE-INDEX DISTRIBUTION. (c) FOCUSING OF LIGHT EMERGING FROM WAVEGUIDE ONTO EXTERNAL SCREEN.

of a lens. We shall present the results of such calculations before discussing our experimental results.

What we wish to describe is the expected light intensity distribution in the focal plane when the guided beam propagation under the central electrode region iii is taken into account as well as propagation in the interelectrode regions i and ii. We assume a uniform beam extending between $-y_o - \Delta y/2$ and $y_o + \Delta y/2$. Then the electric-field distribution in the focal plane is given by

$$E(x) = C \left[\int_{y_o - \Delta y/2}^{y_o + \Delta y/2} \exp\left(-\frac{2\pi i x y}{\lambda f} + \frac{i\eta}{2}\right) dy \right.$$

$$+ \int_{-y_o - \Delta y/2}^{-y_o + \Delta y/2} \exp\left(-\frac{2\pi i x y}{\lambda f} - \frac{i\eta}{2}\right) dy$$

$$\left. + \int_{-y_o + \Delta y/2}^{y_o - \Delta y/2} \exp\left(-\frac{2\pi i x y}{\lambda f}\right) dy \right] , \qquad (14)$$

where C is a complex constant. We have assumed that the beam propagates beneath the electrode without attenuation; under certain circumstances—TM modes, shallow waveguides, electrodes not spaced above the waveguide surface—attenuation may be considerable, particularly for the lowest order mode. The focal-plane intensity distribution $I = E^* E$ is obtained upon evaluating the integrals in (14). We find

$$I(u,\eta) = \kappa\left[\frac{\sin u}{u}\left(\frac{\sin(2Q-1)u}{\sin u} + 2\cos(2Qu-\eta)\right)\right]^2 , \qquad (15)$$

where κ is a real constant; $Q = y_o/\Delta y$; and u is a normalized focal-plane distance:

$$u = \pi \times \Delta y/\lambda f .$$

It is convenient to normalize the intensity to its value at the center of the pattern when the phase shift η is zero. Defining $R(u,\eta)$ as $I(u,\eta)/I(0,0)$, we find readily

$$R(u,\eta) = \left[\frac{\sin(2Q-1)u + 2 \sin u \cos(2Qu-\eta)}{(2Q + 1)u}\right]^2 \tag{16}$$

At the center of the pattern, we have

$$R(0,\eta) = \left(\frac{2Q-1 + 2 \cos \eta}{2Q + 1}\right)^2 \tag{17}$$

from which we see that a minimum at the center of the pattern occurs for a phase shift $\eta = \pi$ (or any odd multiple of π, but obviously $|\eta| = \pi$ requires the smallest applied voltage). Moreover, a complete interference minimum at the pattern center can occur only if $Q \leq 3/2$ or, equivalently, $(M/S) \leq 2$, where M/S is the mark/space ratio of the electrode pattern.

In Fig. 14, we show the calculated normalized focal-plane intensity distribution R as a function of the normalized distance u for Q = 1.5 and for $\eta = \pi$ and $\eta = 0$. For $\eta = \pi$, a voltage has been applied to the electrodes sufficient to cause an interference null at the center of the focal plane. When the electrodes are effectively shorted out by photocarriers excited by the signal beam, $\eta \approx 0$ and we get the strong maximum at the center of the pattern shown in the solid curve. If Q = 2, however, as in Fig. 15, only about a 95% extinction of the central peak is possible.

Considerable leeway in attaining the optimal phase shifts may be allowable. For instance in Fig. 16 we show that a phase shift of 0.8 π radians still produces a fairly good null near u = 0. Likewise, in Fig. 17 we see that a phase shift of 0.1 π radians instead of zero still produces

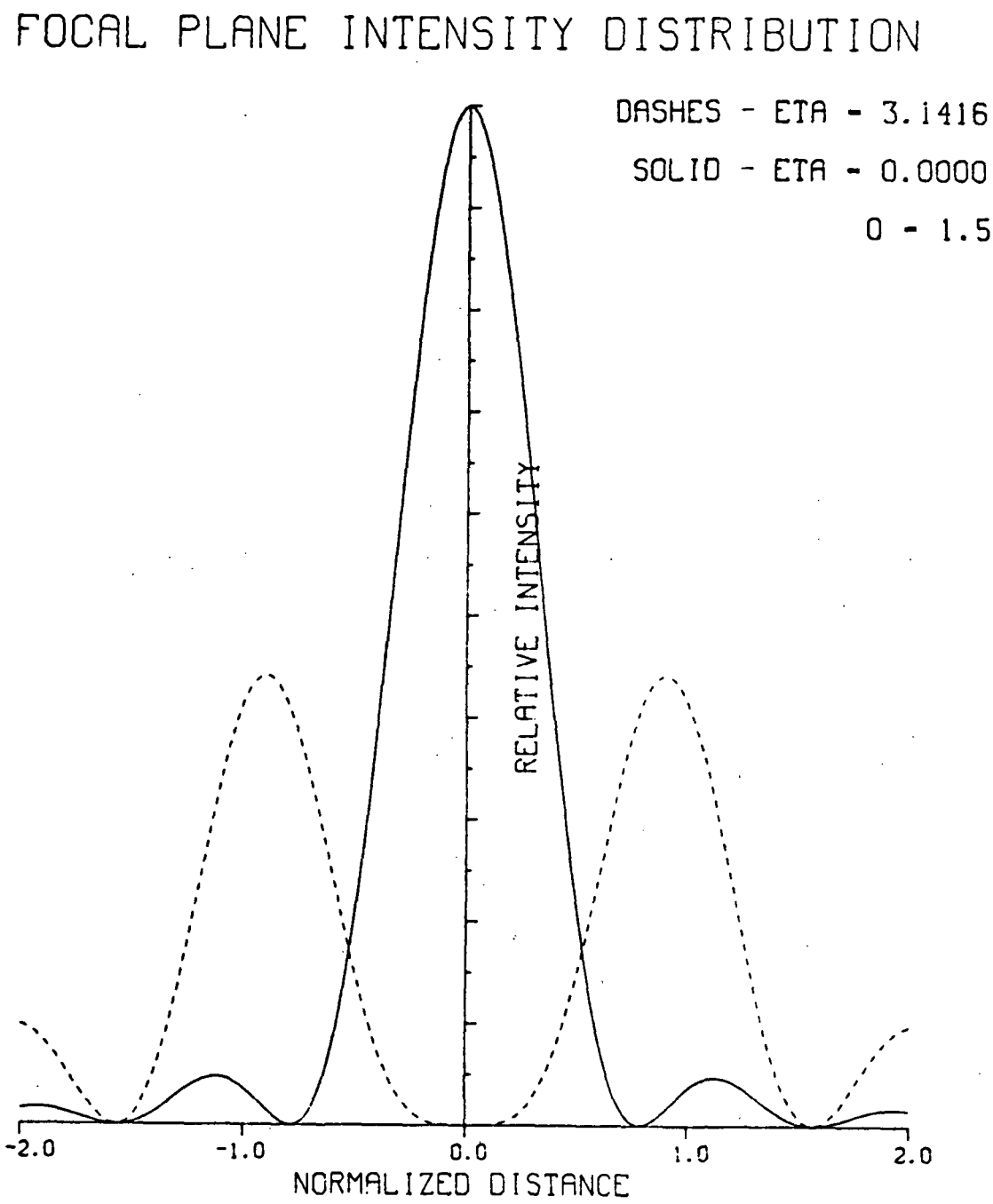

FIGURE 14. CALCULATED OUTPUT OF DEVICE OF TYPE OF FIG. 12. NORMALIZED INTENSITY DISTRIBUTION R AS FUNCTION OF NORMALIZED FOCAL-PLANE DISTANCE u, ILLUSTRATING CENTRAL NULL ATTAINABLE WHEN Q = 1.5, $\eta = \pi$.

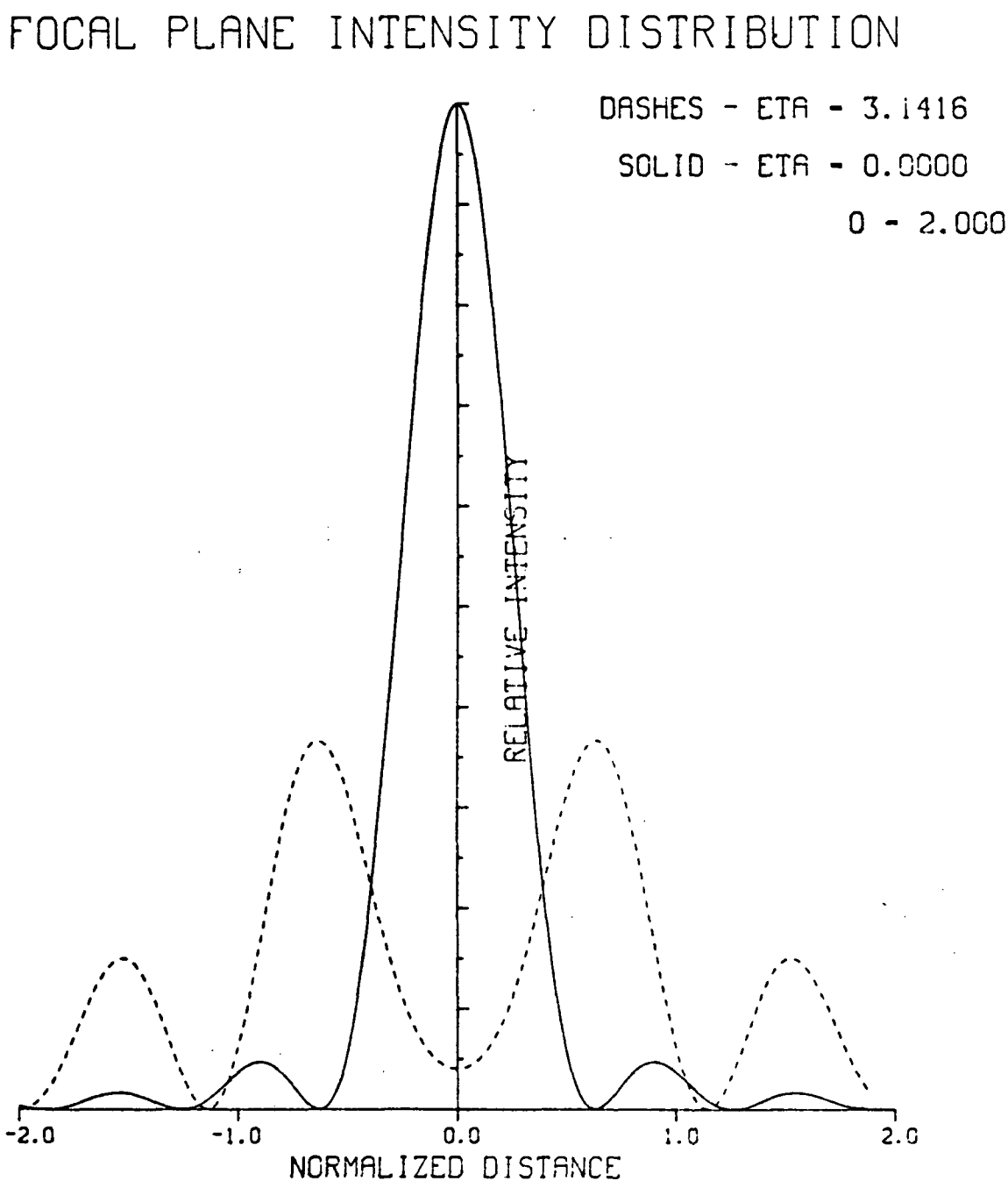

FIGURE 15. CALCULATED OUTPUT OF DEVICE OF FIG. 12 TYPE, ILLUSTRATING IMPERFECT CENTRAL NULL WHEN $Q = 2$, $\eta = \pi$.

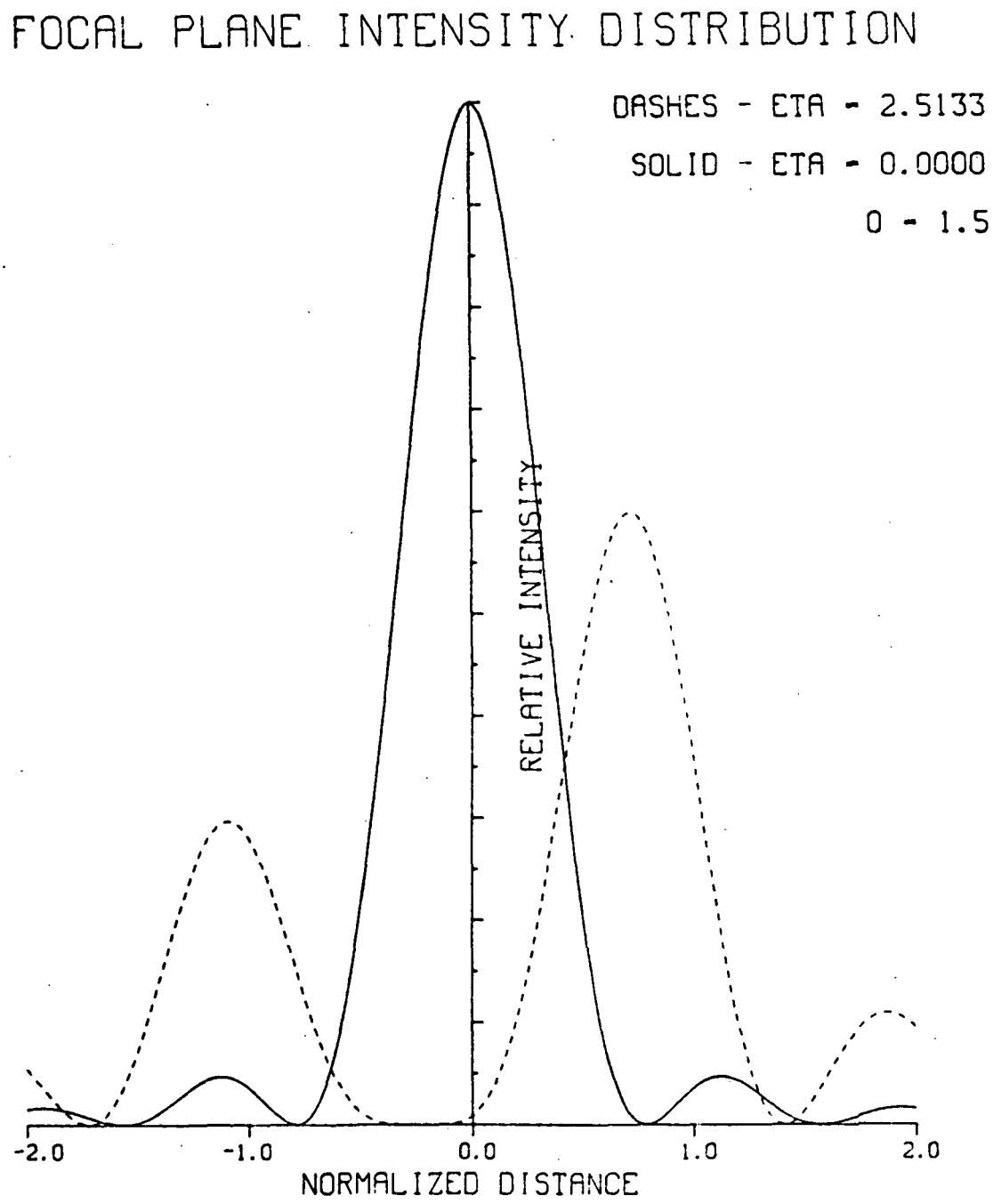

FIGURE 16. CALCULATED OUTPUT OF DEVICE OF FIG. 12 TYPE, ILLUSTRATING NEAR-NULL ATTAINABLE WHEN Q = 1.5, $\eta = 0.8\ \pi$.

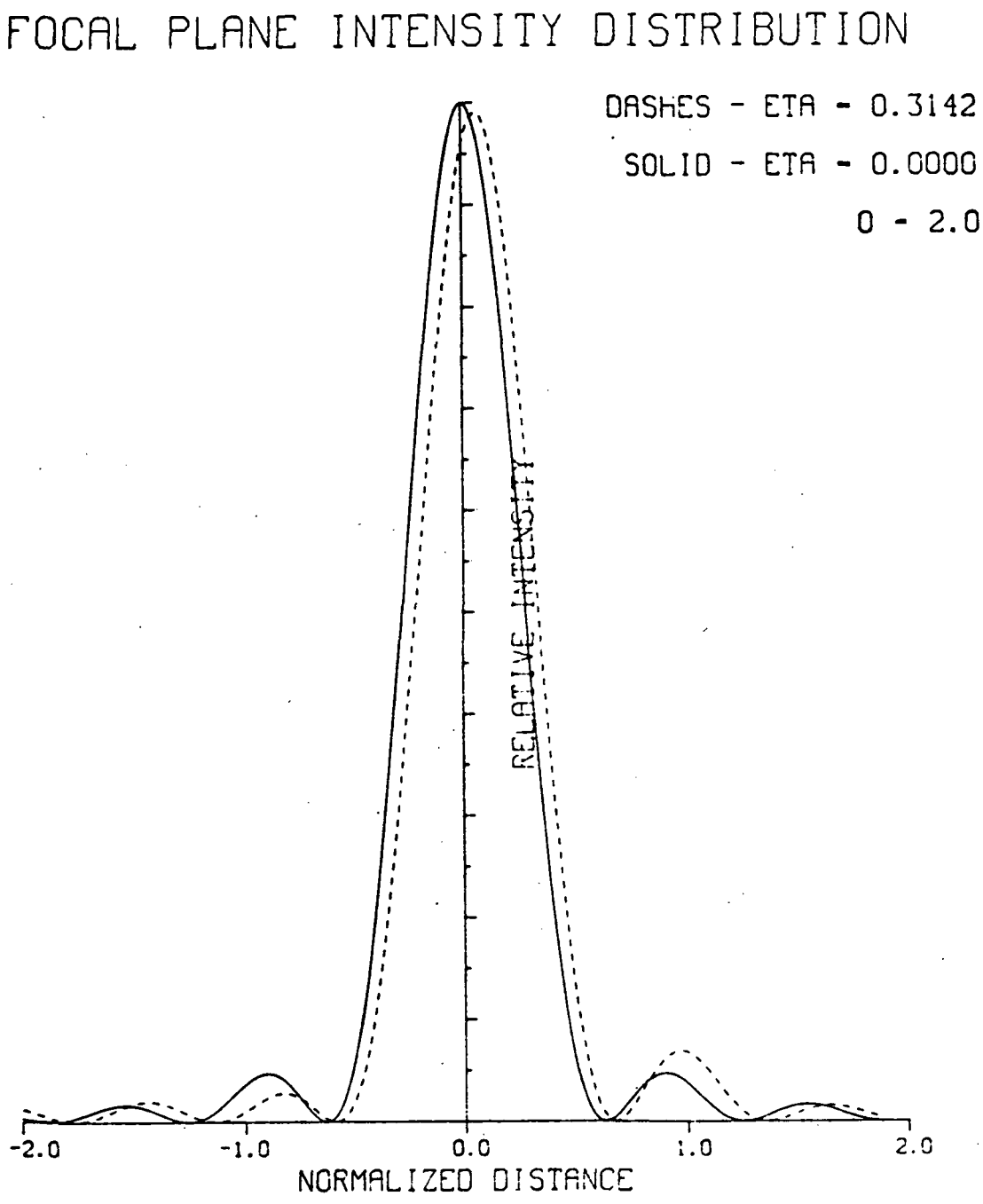

FIGURE 17. CALCULATED OUTPUT OF DEVICE OF FIG. 12 TYPE, ILLUSTRATING NEAR-PEAK ATTAINABLE WHEN Q = 2, $\eta = 0.1\ \pi$.

a sharp central peak. Such behavior is desirable for pulse-code input, but not so good if analog or gray-scale information is to be impressed on the beam. In the latter situation, it is probably best to work in the vicinity of a phase shift of $\pi/3$, where the change in $R(0,\eta)$ with η is greatest. A reduced dynamic range must, however, be allowed for.

The remainder of the experimental work was largely devoted to determining the optimum operating conditions for the device. This work was done using the inexpensive photocells on hand, but similar design princples should be applicable to any devices of the same general type.

To estimate the voltage which must be applied to the electrodes to obtain the maximum effect, that is, to produce a phase shift $\eta = \pi$, we used the calculations of Vandenbulcke and Lagasse[33] for the electric field produced by surface electrodes in $LiNbO_3$, ignoring the fact that our electrodes are spaced away from the $LiNbO_3$ by a plastic layer. The switching voltage was estimated at 200 V. By interfering the beam passing through the waveguide with an external beam, we determined holographically that the voltage required was indeed in the 200-300 V range.

A simple equivalent circuit for the photocell and its power supply is indicated in Fig. 18. The limiting resistor R_L is necessary to prevent current-overload damage to the photocell when it is illuminated. It is also useful for increasing the change in electrode potential between the dark ("off") and illuminated ("on") states. The effective cell capacitance C will be much greater in the on-state than the simple electrode capacitance because of space-charge effects. Strictly speaking, it, as well as the photoresistance R_{ph}, will depend on the illumination intensity. Sufficient light from the waveguide beam leaks into the photocell that

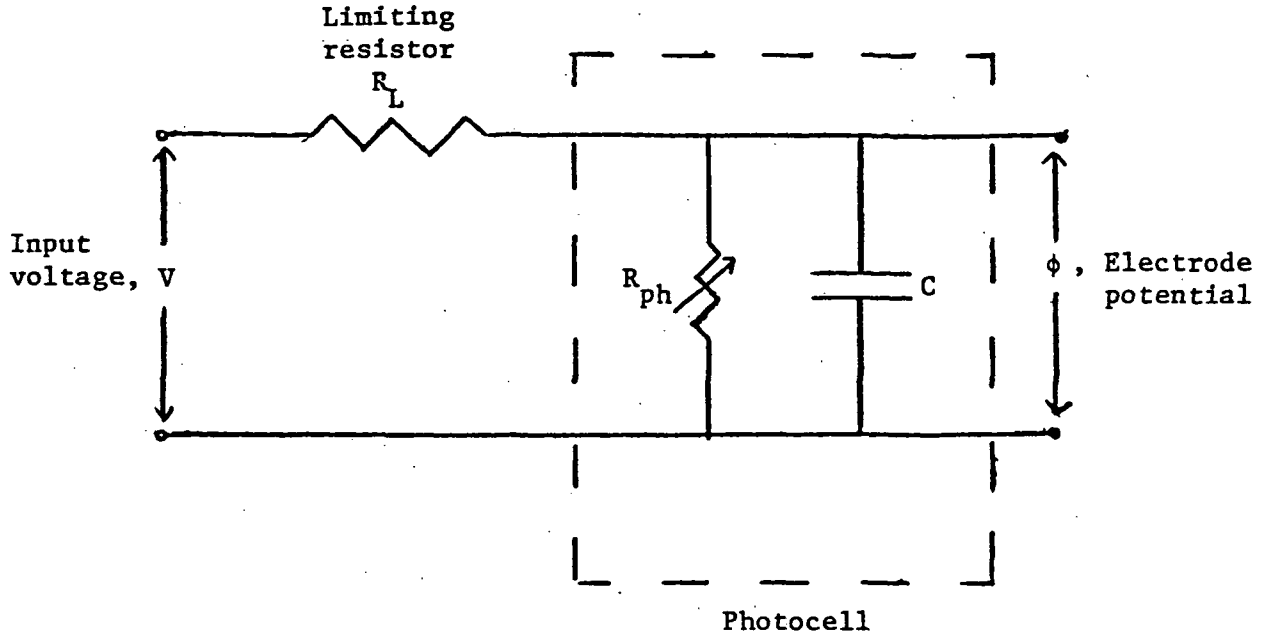

FIGURE 18. SIMPLIFIED EQUIVALENT CIRCUIT MODEL FOR PHOTOCELL AND SUPPLY FOR DEVICE OF FIG. 12. THE PHOTORESISTANCE R_{ph} DECREASES ON ILLUMINATION WITH THE SIGNAL BEAM.

its resistance in the off-state is considerably reduced from what it would be in complete darkness. A typical measured value is $R_{ph}^{d} = 160$ kΩ. Upon illumination with about 4 mW/cm^2 of incandescent light, this resistance drops typically to $R_{ph}^{\ell} = 6$ kΩ. We estimate that no more than half the incandescent-light energy incident is absorbed; of this only around 3% is effective in creating photocarriers.

If the signal beam is turned on at t = 0, the potential for the phase-shift electrodes will evolve according to

$$\phi = VR_L^{-1}\left[R_{||}^{\ell} + (R_{||}^{d} - R_{||}^{\ell})\exp(-t/R_{||}^{\ell}\, C)\right] \quad , \tag{18}$$

where

$$R_{||}^{-1} = R_L^{-1} + R_{ph}^{-1} \quad .$$

Clearly we need $R_L > R_{ph}^{\ell}$, or the turn-on time $R_{||}^{\ell}C$ will be increased unduly. However if, as would usually be the case, the power supply has a high back-bias resistance, the turn-off or decay time in the dark will be controlled by R_{ph}^{d}, and this may often control the overall cycle time since it takes a while to reach its maximum value. In any event, R_L must also be large enough that the maximum allowable cell current i_A (7.5 mA for our cells) is not exceeded; thus

$$R_L > V\, i_A^{-1} - R_{ph}^{\ell} \quad . \tag{19}$$

A large R_L is also desirable for getting the maximum ratio of electrode potentials between the off and on states; if this potential is ϕ_o in the off state and ϕ_∞ in the on state,

$$\frac{\phi_o}{\phi_\infty} = \frac{R_{ph}^{d}}{R_{ph}^{\ell}} \frac{(R_L + R_{ph}^{\ell})}{(R_L + R_{ph}^{d})} \qquad (20)$$

If R_L is too large, however, the supply voltage needed may be unacceptably high. The interference-pattern calculations described above indicate a minimum acceptable ratio ϕ_o/ϕ_∞ of about 5; so for the R_{ph} values given previously, Eq. (20) shows we need $R_L \geq 30$ kΩ. Since the potential ϕ_o required to produce the desired phase shift of π radians was found to be of the order of 250 V, we see from Eq. (18) that an applied voltage V of 297 V is required. We then find from Eq. (19) that the rated current i_A will be exceeded by about 10%, though. It will be necessary, therefore, to increase R_L by something more than 10% since the applied voltage needed to get $\phi_o \approx 250$ V will also increase with R_L.

Upon performing some experiments in which R_L was varied in the range 60 kΩ to 300 kΩ, we found that the potentials on the electrodes in both off and on states were very close to those expected. Two difficulties were encountered in these experiments. First, the expected magnitude of fringe shift on illumination did not occur when a chopped (1/7 sec on, 6/7 sec off) incandescent beam was used. This appeared to be chiefly a problem of fringe visibility rather than of photocell response, but might merit futher investigation. Second, when a steady incandescent beam was used, a long-term fringe drift apparently indicating a sample temperature change, was observed. The device is rather isolated thermally in its present configuration and is thus cooled predominantly by radiation and free convection. The input power which must be dissipated by these mechanisms is given by

$$P_{in}^{d} = \phi_o^2 \, (R_{ph}^{d})^{-1} + P_{coh} \tag{21}$$

in the off state and by

$$P_{in}^{\ell} = \phi_\infty^2 \, (R_{ph}^{\ell})^{-1} + P_{coh} + P_{inc} \tag{22}$$

in the on state, where P_{coh} is the power absorbed from the coherent waveguide beam and P_{inc} is that absorbed from the incoherent signal beam. Since the spot size is about 1 cm^2, P_{inc} is 2 mW at most. For R_L = 100 kΩ and ϕ_o = 250 V, the electrical input power is about 370 mW in the off state and about 70 mW in the on state; so the device tends to cool off when the signal beam is turned on. It is not hard to show that this effect can in principle be reduced by reducing the limiting resistance to the 30-40 kΩ range; then after an initial warm-up period the device would remain at close to the same temperature whether the signal beam was on or off, provided of course that the ambient conditions did not vary, but this conclusion has not been checked experimentally.

To transform a laboratory device of the type discussed here into a practical DOI system, it would be necessary to replace the external lens and detector with an integrated lens and detector array and to allow for the presence of many parallel information channels, rather than a single one. Since a simply-produced spherical geodesic lens will have fairly good focusing properties over a large aperture[34], some means for spatially separating the information-channel focal points must be provided. Two possibilities are:

i) Use an intentionally aberrated lens or lens system. A thin electrooptic overlay lens[15] in combination with a spherical geodesic lens might suffice.

ii) Place a large-aperture long focal-length geodesic lens before the electrode pattern so the focusing lens is addressed by a convegent beam.

It would also be necessary, of course, to design and deposit one's own electrode patterns and photoconductor regions. Depositing CdS on $LiNbO_3$ in such a way that it will have the desired photoconducting properties is a rather difficult process,[35] however, and, we did not attempt it on the present program.

Many other possible device modifications will doubtless occur to the reader. For one example, the lenses could be eliminated altogether and the whole pattern emerging from the electrode region caused to interfere with another guided plane wave. If the input data were in a suitable optical form, such an arrangement could be used to provide DOI to an integrated-optical holographic data preprocessor such as we are developing for NASA under a parallel program.

CONCLUSIONS

We have described a variety of device concepts for direct optical input to integrated-optical data-processing devices and have demonstrated one experimentally. Several of the concepts appear to be workable with known materials, but whether they will ever find application depends on the existence of "suitable" input data—that is, optical signals of proper wavelength, intensity, and frame rate—on which useful optical processing operations can be performed. We have tried to outline DOI device design concepts in a general way, so that additional device ideas oriented towards particular applications can be readily generated. One of the principal factors determining the ultimate utility of any device will be the compatibility of the waveguide material used for DOI with the ultimate data-processing device. Ideally devices will be integrated with one another so that DOI and ODP functions will be performed on the same chip. But the range of materials carefully explored for use in integrated optics is remarkably small, while the general support for the concept of heterogeneous integrated-optic devices appears to be declining. Thus the prospective user of DOI is going to be faced not only with selection and optimization of a suitable DOI device along the lines described in the present report, but also with problems of materials development or systems development or both.

We conclude with several comments relative to future work in this area:

1) Future research should address the development and design of overall integrated-optics systems with DOI for specific data-processing tasks on input signals of known characteristics,

2) Feedback devices, both with amplification[1-3] and without, (ref. 4 and previous discussion in this report) deserve more detailed analysis.

3) Reliability and expected service life will have to be carefully evaluated for systems proposed for use in the field.

REFERENCES

1. P. W. Smith, I. P. Kaminow, P. J. Maloney, and L. W. Stulz, "Integrated Bistable Optical Devices", Appl. Phys. Lett. 33 (1), 24-26 (1978).

2. P. S. Cross, R. V. Schmidt, R. L. Thornton, and P. W. Smith, "Optically Controlled Two Channel Integrated-Optical Switch", IEEE J. Quantum Electron. QE-14 (8), 577-580 (1978).

3. E. Garmire, S. D. Allen, J. Marburger, and C. M. Verber, "Multimode Integrated Optical Bistable Switch", Optics Letts. 3 (2), 69-71 (1978).

4. P. W. Smith, I. P. Kaminow, P. J. Maloney, and L. W. Stulz, "Self-Contained Integrated Bistable Optical Devices", Appl. Phys. Lett. 34 (1), 62-65 (1978).

5. J. P. Huignard, F. Micheron, and E. Spitz, "Optical Systems and Photosensitive Materials for Information Storage", in Optical Properties of Solids, New Developments, B. O. Seraphin, ed., pp. 847-925 (North-Holland Publishing Co., Amsterdam, 1976).

6. B. Hill, "Holographic Memories and Their Future", Advances in Holography 3, N. H. Farhat, ed. (Marcel Dekker, Inc., New York, 1976).

7. V. V. Voronov, Yu. S. Kuz'minov, and V. V. Osiko, "Optically Induced Changes in the Refractive Index of Ferroelectric Crystals and their Use in Reusable Holographic Memories (Review)", Sov. J. Quantum Electron. 6 (10), 1143-1157 (1976).

8. H. M. Smith, ed., Holographic Recording Materials, Topics in Applied Physics 20 (Springer-Verlag, Berlin, 1977).

9. C.-L. Chen, "Integrated Optic Modulators", in Proceedings First Fiber Optics and Communications Exposition, M. A. O'Bryant and P. Polishuk, eds., pp 142-147 (Information Gatekeepers, Inc., Brookline, MA, 1978).

10. M. Peltier and F. Micheron, "Volume Hologram Recording and Charge Transfer Process in $Bi_{12}SiO_{20}$ and $Bi_{12}GeO_{20}$", J. Appl. Phys. 48 (9), 3683-3690 (1977).

11. A. A. Ballman, H. Brown, P. K. Tien, and R. J. Martin, "The Growth of Single Crystalline Waveguiding Thin Films of Piezoelectric Sillenites", J. Cryst. Growth 20, 251-255 (1973).

12. H. Hayashi and Y. Fujii, "Programmable Optical Guided-Wave Device Using $Bi_{12}SiO_{20}$ Crystal", IEEE J. Quantum Electron. QE-14 (11), 848-854 (1978).

13. F. Micheron, "Sensitivity of the Photorefractive Process", Ferroelectrics 18, 153-159 (1978).

14. Y. Ohmachi and T. Igo, "Laser-Induced Refractive-Index Change in As-S-Ge Glasses", Appl. Phys. Lett. 20 (12), 506-508 (1972).

15. D. W. Vahey, "Corrected Waveguide Geodesic Lenses for Integrated Acoustooptic Spectrum Analysis", in 1978 Ultrasonic Symposium Proceedings, J. deKlerk and B. R. McAvoy, eds., pp 70-73 (IEEE, New York, 1978).

16. L. Goldberg and S. H. Lee, "Optically Activated Switch/Modulator Using a Photoconductor and Two Channel Waveguides", Radio Sci. 12 (4), 537-542 (1977).

17. L. B. Schein, P. J. Cressman, and L. E. Cross, "Pyroelectric Induced Optical Damage in $LiNbO_3$", J. Appl. Phys. 49 (2), 798-800 (1978).

18. M. Masuda and J. Koyama, "Effects of a Buffer Layer on TM Modes in a Metal-clad Optical Waveguide Using Ti-diffused $LiNbO_3$ C-plate", Appl. Opt. 16 (11), 2994-3000 (1977)..

19. I. Balberg and S. Trokman, "High-contrast Optical Storage in VO_2 Films", J. Appl. Phys. 46 (5), 2111-2119 (1975).

20. J. R. Carruthers, I. P. Kaminow, and L. W. Stulz, "Outdiffusion Kinetics and Optical Waveguiding Properties of Outdiffused Layers in Lithium Niobate and Lithium Tantalate", Appl. Opt. 13 (10), 2333-2342 (1974).

21. G. B. Hocker, "Strip-Loaded Diffused Optical Waveguides", IEEE J. Quantum Electron. QE-12 (4), 232-236 (1976).

22. R. A. Sprague and P. Nisenson, "The PROM-A Status Report", Opt. Eng. 17 (3), 256-266 (1978).

23. T. Mitsuyu, K. Wasa, and S. Hayakawa, "RF-Sputtered Epitaxial Films of $Bi_{12}TiO_{20}$ on $Bi_{12}GeO_{20}$ for Optical Waveguiding", J. Cryst. Growth 41 , 151-156 (1977).

24. H. Naitoh, S. Noda, K. Muto, and T. Nakayama, "Mirror-type Optical Switch Array", Appl. Opt. 17 (24), 3975-3978 (1978).

25. S. K. Sheem and C. S. Tsai, "Light Beam Switching and Modulation Using a Built-in Dielectric Channel in $LiNbO_3$ Planar Waveguide", Appl. Opt. 17 (6), 892-894 (1978).

26. B. Goldstein and L. Pensak, "High-Voltage Photovoltaic Effect", J. Appl. Phys. 30 (2), 155-161 (1959).

27. P. S. Brody, "Temperature Dependence of the Short-Circuit Photocurrent in Ferroelectric Ceramics", Ferroelectrics 10, 143-146 (1976).

28. H. F. Taylor, M. J. Taylor, and P. W. Bauer, "Electro-optic Analog-to-Digital Conversion Using Channel Waveguide Modulators", Appl. Phys. Lett. 32 (9), 559-561 (1978).

29. V. Ramaswamy, M. D. Divino and R. D. Stanley, "Balanced Bridge Modulator Switch Using Ti-diffused $LiNbO_3$ Strip Waveguides", Appl. Phys. Lett. 32 (10), 644-646 (1978).

30. R. P. Kenan, C. M. Verber and Van E. Wood, "Wide-Angle Electro-optic Switch", Appl. Phys. Lett. 24 (9), 428-430 (1974).

31. C. S. Tsai and P. Saunier, "Ultrafast Guided-Light Beam Deflection/Switching and Modulation Using Simulated Electro-optic Prism Structures in $LiNbO_3$ Waveguides", Appl. Phys. Lett. 27 (7), 248-250 (1975).

32. I. P. Kaminow and L. W. Stulz, "A Planar Electrooptic-Prism Switch", IEEE J. Quantum Electron. QE-11 (8), 633-635 (1975).

33. P. Vandenbulcke and P. E. Lagasse, "Static Field Analysis of Thin Film Electrooptic Light Modulators and Switches", Wave Electron. 1, 295-308 (1974-76).

34. T. van Duzer, "Lenses and Graded Films for Focusing and Guiding Acoustic Surface Waves", Proc. IEEE 58 (8), 1230-1237 (1970).

35. P. G. Kornreich, A. Mahapatra, S. T. Kowel, K. W. Loh, and B. Emmer, "Double-Layered Polycrystalline Cadmium Sulfide on Lithium Niobate", J. Appl. Phys. 49 (4), 2443-2448 (1978).

1. Report No.	2. Government Accession No.	3. Recipient's Catalog No.
NASA-CR-159054		

4. Title and Subtitle	5. Report Date
Study of Methods for Direct Optical Address of Integrated Optical Circuits	June 15, 1979
	6. Performing Organization Code
7. Author(s)	8. Performing Organization Report No.
V. E. Wood and C. M. Verber	
	10. Work Unit No.
9. Performing Organization Name and Address	11. Contract or Grant No.
Battelle Columbus Laboratories 505 King Avenue Columbus, Ohio 43201	NAS1-15315
	13. Type of Report and Period Covered
12. Sponsoring Agency Name and Address	Contractor Report
National Aeronautics and Space Administration Washington, DC 20546	14. Sponsoring Agency Code

15. Supplementary Notes

Technical Monitor: Marvin E. Beatty III, NASA Langley Research Center

16. Abstract

Methods for introducing optical information directly, without intervening recording and storage steps, into integrated optical data-processing devices are surveyed. The information is taken to be in the form of a one-dimensional variation of intensity across the beam. Physical phenomena that may be utilized, including photorefractive, photochromic, thermooptic, photoconductive, and photovoltaic effects, are evaluated, and the most suitable presently known classes of materials for exploitation of each type of interaction are discussed. A variety of possible device configurations utilizing various interaction phenomena are suggested and general principles are outlined whereby many more device types can be generated. While many plausible methods for direct optical input can be outlined, none can be said to be generally superior, in part because the most feasible scheme for a given application will be strongly dependent on the nature of the input signal and the data-processing operations to be carried out, and in part because of uncertainties concerning the ultimate capabilities of the various classes of photosensitive materials and concerning the compatibility of different optical waveguide materials. A simple experimental device was demonstrated and its operation was analyzed. It involves differential electrooptic phase modulation in pairs of parallel waveguide channels through absorption of signal beam light in a photoconductive surface layer. The phase modulation was converted to an intensity modulation by using an external lens.

17. Key Words (Suggested by Author(s))	18. Distribution Statement
Integrated optics Optical data processing Optical waveguides Optical modulators Incoherent-coherent conversion Photoconductivity	Unlcassified - Unlimited

19. Security Classif. (of this report)	20. Security Classif. (of this page)	21. No. of Pages	22. Price*
Unclassified	Unclassified	59	

* For sale by the National Technical Information Service, Springfield, Virginia 22161